Journal of the European Ceramic Society **6** (1990) 205–225

State of the Art

Boron Carbide—A Comprehensive Review

Francois Thévenot

Ecole Nationale Supérieure des Mines de Saint-Etienne, 158, cours Fauriel, 42023 Saint-Etienne, Cédex 2, France

(Received 3 October 1989; revised version received 18 April 1990; accepted 3 May 1990)

Abstract

Boron carbide, which has a high melting point, outstanding hardness, good mechanical properties, low specific weight, great resistance to chemical agents and high neutron absorption cross-section ($^{10}B_xC$, $x>4$) is currently used in high-technology industries—fast-breeders, lightweight armors and high-temperature thermoelectric conversion.

The contents of this review are: (1) introduction; (2) preparations—industrial preparative routes, powders, sintering (additives, pressureless, hot pressing, HIP); laboratory methods of synthesis (CVD, PVD, plasma, crystal growth); (3) analytical characterization; (4) phase diagram—a peritectic, nearly pure boron, and a wide phase homogeneity range (B_4C–$B_{10.5}C$); (5) rhombohedral crystal structure—a comprehensive model of the whole solid solution is proposed; (6) chemical properties; (7) physical properties—density, mechanical (strength, hardness, toughness) and thermo-electrical properties; (8) main industrial applications; (9) conclusion.

Borcarbid wird zur Zeit auf Grund seines hohen Schmelzpunkts, seiner außergewöhnlichen Härte, seiner guten mechanischen Eigenschaften, seines geringen spezifischen Gewichts, seiner hohen Korrosionsbeständigkeit und seines Neutroneneinfangquerschnitts ($^{10}B_xC$, $x>4$) für spezielle Anwendungen in der Industrie—den schnellen Brüter, für Panzerungen mit geringem Gewicht und für Hochtemperaturthermoelemente—eingesetzt. Diese Zusammenfassung gliedert sich wie folgt: (1) Einleitung; (2) Herstellung—industrielle Herstellungsmethoden, Pulver, Sintern (Additive, drucklos, Heißpressen, HIP); labormäßige Herstellungsverfahren (CVD, PVD, Plasma, Kristallzüchtung); (3) Analytische Untersuchungen; (4) das Phasendiagramm—ein Peritektikum in der Nähe reinen Bors und ein weiter Homogenitätsbereich B_4C–$B_{10}C$; (5) die rhomboedrische Kristallstruktur—ein umfassendes Modell der gesamten Mischkristallbildung wird vorgeschlagen; (6) die chemischen Eigenschaften; (7) die physikalischen Eigenschaften—Dichte, mechanische (Festigkeit, Härte, Zähigkeit) und thermoelektrische Eigenschaften; (8) die industriellen Hauptanwendungsgebiete; (9) Zusammenfassung.

Le carbure de bore, qui présente un haut point de fusion, une dureté remarquable, de bonnes propriétés mécaniques, une faible masse volumique, une grande résistance aux milieux chimiques agressifs et une section efficace d'absorption neutronique élevée ($^{10}B_xC$, $x>4$) est couramment employé dans les domaines technologiques de pointe suivants—surgénérateurs, blindages légers et convertisseurs thermoélectriques à haute température.

Cet article traite des thèmes suivants: (1) introduction; (2) préparation—voies de préparation industrielles, poudres, frittage (additifs, frittage naturel, pressage à chaud, HIP); méthodes de synthèse en laboratoire (CVD, PVD, plasma, croissance cristalline); (3) caractérisation analytique; (4) diagramme de phases—péritectique au voisinage du bore pur et domaine étendu d'homogénéité de la phase (B_4C–$B_{10.5}C$); (5) structure cristalline rhombohédrique—un modéle général pour la totalité de la solution solide est proposé; (6) propriétés chimiques; (7) propriétés physiques—densité, propriétés mécaniques (résistance mécanique, dureté, ténacité) et propriétés thermoélectriques; (8) principales applications industrielles; (9) conclusion.

1 Introduction

In the group of the most important non-metallic hard materials (alumina, silicon carbide, silicon

Journal of the European Ceramic Society 0955-2219/90/$3.50

nitride, diamond or cubic boron nitride), boron carbide occupies a specific place.

A boron carbide compound was discovered in 1858,[1] then Joly in 1883 and Moissan in 1894 prepared and identified the compounds B_3C and B_6C, respectively. The 'stoichiometric formula' B_4C was only assigned in 1934.[2] Then many diverse formulae were proposed by Russian authors, which have not been confirmed; in fact, there is a wide phase homogeneity range $B_{4\cdot0}C$–$B_{10\cdot5}C$ (cf. Section 4). After 1950, numerous studies were carried out, especially concerning structures and properties. Due to the limited size of this review, only some of the most important or recent references and the more appropriate reviews[1,3–8] will be cited.

The different topics given in the abstract will be described here.

2 Preparative Routes

2.1 Industrial preparation of boron carbide powders[1,3,6,8,9]

Annual production in the non-communist countries is about 500 tons[6]

2.1.1 Reduction of boron anhydride (or acid) with carbon

The overall reaction is written:

$$2B_2O_3 + 7C \rightarrow B_4C + 6CO \qquad (1)$$

The process is strongly endothermic ($\Delta H =$ 1812 kJ/mol or 9·1 kWh/kg)[6] and takes place in two stages:

$$B_2O_3 + 3CO \rightarrow 2B + 3CO_2 \qquad (2)$$

$$4B + C \rightarrow B_4C \qquad (3)$$

Brickets of the B_2O_3–C mixture are placed in an electric-arc furnace. The central zone reaches 2473–2773 K and gives a carbide of composition near $B_{4\cdot3}C$, containing a few percent free graphite. The melted carbide is then crushed and milled to produce the grain size appropriate for final use (Fig. 1). The pollution introduced during milling is eliminated by acid leaching. The outer zones of the furnace are less hot (1473–2473 K) and contain unreacted products, which must be recycled.

A graphite-tube furnace may also be used at 1973–2073 K, under a protective atmosphere; a stoichiometric, fine-grained boron carbide (0·5–5 μm) is obtained, but the yield is lower than in the case of arc-melting.

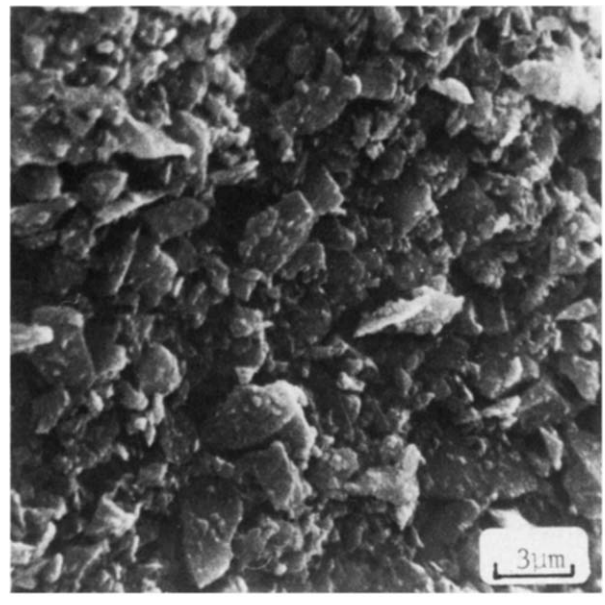

Fig. 1. Arc-melted powder; mean grain size $<5\,\mu$m; specific surface $\approx 10\,m^2/g$.

2.1.2 Reduction of boron anhydride with magnesium in the presence of carbon black

The reaction is strongly exothermic:

$$2B_2O_3 + 6Mg + C \rightarrow B_4C + 6MgO \qquad (4)$$

A furnace may be used at 1273–1473 K or directly after initiating by a point ignition; reaction (4) is strongly exothermic. To eliminate magnesia, borides (MgB_2, etc.) and unreacted Mg metal, the final product is washed with H_2SO_4, or HCl, then with hot water. A stoichiometric carbide with low granularity (0·1–5 μm) is obtained directly (Fig. 2). It is possible to prepare graphite-free material; in other cases, it may contain 2% graphite.

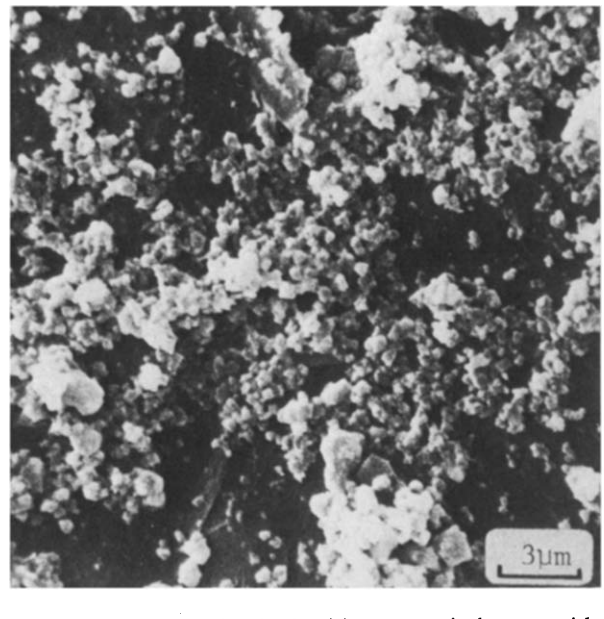

Fig. 2. Powder directly obtained by magnesiothermy, without milling; mean grain size $<2\,\mu$m; specific surface $\approx 21\,m^2/g$.

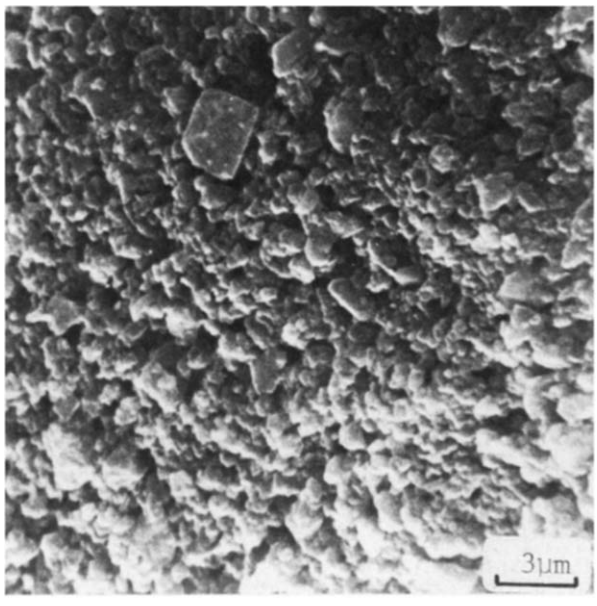

Fig. 3. Magnesiothermal powder purified by a vacuum heat treatment then milled; mean grain size $< 5\,\mu m$; specific surface $\approx 11\,m^2/g$.

After heat treatment of this powder under vacuum (1600°C, 10^{-2} mbar, 2 h), free carbon, nitrogen and magnesium are eliminated. During heat treatment, the specific surface is drastically decreased from $21\,m^2/g$ in the initial powder to $5\,m^2/g$ after 1 h at 1600°C. The resulting powder is milled by attrition, and the steel pollution eliminated by HCl leaching; the purified powder is shown in Fig. 3.[10–12]

A soluble carbohydrate that decomposes to carbon may be used with the carbon black.[13]

2.2 Sintering of boron carbide powders

The following different methods of sintering boron carbide powders to prepare dense materials are discussed:

(1) Hot pressing (and hot isostatic pressing);
(2) pressureless sintering:
  (a) using metallic, inorganic, etc., additives;
  (b) adding carbon obtained by pyrolysis of an organic precursor—phenolic resin (alone or with polycarbosilane).

Two recent reviews on sintering have been prepared[9,14] so only the more recent references will be cited here.

2.2.1 Hot pressing of boron carbide

2.2.1.1 Hot pressing of stoichiometric $B_{4\cdot0}C$ (20 at.%C). Hot pressing (HP) is used industrially to prepare different simple shapes. Boron carbide is hard and can be machined only using diamond (or BN_c) rectification. To obtain dense

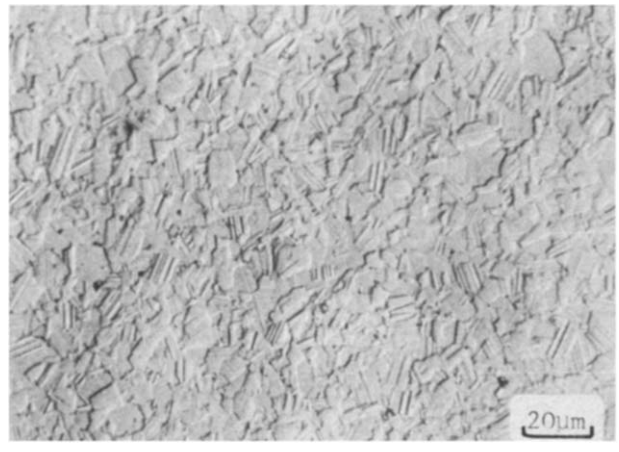

Fig. 4. Hot-pressed sample; mean grain size $\approx 5\,\mu m$; twins are present.

products under vacuum or inert atmosphere: (1) fine and pure powders ($< 2\,\mu m$); (2) high temperatures (2373–2473 K); (3) pressures of 30–40 MPa; and (4) 15–45 min of pressing in graphite dies should be used. The density, porosity and microstructure (Fig. 4) depend on the sintering parameters.[15]

Densification by sintering during HP results from three successive mechanisms: (1) particle rearrangement, where the enclosed porosity is constant and low; (2) plastic flow, leading to the closing of open porosity; or (3) decrease by volume diffusion of the closed porosity by pore elimination at the end of the HP.

2.2.1.2 Hot pressing of boron-rich carbides (2273–2373 K, 20–40 MPa, vacuum or inert atmosphere, 30–60 min). The limits of the rhombohedral boron carbide phase are: B_4C (20 at.%C) to $B_{10\cdot5}C$ (8·8 at.%C) (cf. Section 4). HP of these compounds is a delicate operation. Extensive carbon diffusion takes place from the mold toward the sample and the sintering of pure boron produces only boron carbide.[16] The diffusion diagram in the B–C system has been established.[17,18] Refractory metallic foils (Ta, Mo, W, etc.) can be used for protection. By using a boron nitride barrier (HP or deposited onto graphite mold and punches) it is possible to prepare dense and pure boron and boron-rich phases (between $B_{10\cdot5}C$ and B_4C) by HP in graphite dies.[17,18] The models of densification kinetics of boron carbides have been determined.[17,19,20] Carbon-rich boron carbides have the lowest viscosity and are more easily densified than the boron-rich materials.[17,20]

2.2.1.3 Hot pressing with additions.[9] The use of dopants has different purposes: (1) lowering the densification temperature (complete densification at

2023–2173 K); (2) increasing the oxidation and thermal-shock resistance; (3) hindering grain growth, thus improving mechanical properties. But the problem of purity remains: the material is not convenient for nuclear applications.

Doping agents include: (1) the pure elements: Mg, Al, V, Cr, Fe, Co, Ni, Cu—and recently Si and Ti;[21,22] (2) different compounds: glass, BN, MgO, Al_2O_3, sodium silicate + $Mg(NO_3)_2$ and Fe_2O_3, ethyl silicate, MgF_2 or AlF_3.

2.2.2 Hot isostatic pressing of boron carbide

This promising new technique, using glass encapsulation, without any additive, gives high-density samples at a low temperature: (1700°C).[23] Hot isostatic pressing (HIP) (1200–1750°C, 700–3000 bar) of B_4C in the presence of excess B, C, N using molds of Ti or Zr, avoids the problem of graphite diffusion: owing to the formation of compounds of higher melting points than that of the mold material between the mold and boron carbide, leaks were prevented.[24,25]

Pressureless sintered B_4C materials ($d = 93$–97%) which were doped with 1–3 wt% C (as described in Section 2.2.6) are then treated by HIP (post-HIPped) without encapsulation at 2000°C under an Ar gas pressure of 200 MPa, for 2 h: post-HIPping treatment gives final densities of >99%. Residual porosity was eliminated: mechanical properties and wear resistance were improved. There is a more frequent presence of twins in 'HIPped' samples than in HP; the SEM micrographs show almost 100% transgranular fracture.[26]

2.2.3 Microwave sintering of boron carbide.[27,28]

Boron carbide is sintered to 0·95 d_{th} in less than 12 min without sintering aids by heating to 2000°C with 2·45 GHz microwave radiation. A mean grain size of 20 μm results, twins and microcracking are present. Energy usage for microwave sintering was found to be 18% less than for inductive HP.

2.2.4 Explosion[29,30]

The type of method is of no significant importance.

2.2.5 Pressureless sintering of boron carbide

2.2.5.1 Pressureless sintering without additive.[9,14]

Boron carbide possesses strong bonding, low plasticity, high resistance to grain boundary sliding and low superficial tension in the solid state, all factors that hinder sintering. Sintering parameters under an inert atmosphere are known for a wide phase homogeneity range, $B_{8\cdot3}$–$B_{4\cdot1}C$.[31] The conditions for dense products are: (1) boron carbide powders are preferred (reaction sintering gives porous material); (2) the grain size must be as low as possible, <3 μm (powders with sizes larger than 8 μm cannot be sintered); (3) higher temperatures (2523–2553 K), near the melting boron carbide point of (2573–2623 K) are needed.

During sintering recrystallization starts at 2073 K and at >2273 K grains grow rapidly. The resulting twinning can be removed by high-temperature annealing.[32,33] The impurity-induced activation of the sintering of industrial B_4C arises from the formation of low-melting borides;[34] the impurities evaporate during sintering.

2.2.5.2 Pressureless sintering with inorganic and metallic additions.[9,14] A lot of inorganic additives have been proposed:

(1) For sintering at <2073 K: Cr, Co, Ni, glass and alumina with final density <78%.
(2) For higher temperatures (2423–2523 K): Si, Al, Mg, TiB_2, CrB_2, Al, SiC, Be_2C and more recently, SiC + Al,[35] B + C,[10] B + Si (up to 20 at.% Si),[21,22] W_2B_5,[36] TiB_2 + C[37], Al or TiB_2 or AlF_3[38] additions have improved the densification; but an exaggerated grain growth, a low mechanical strength, and a high impurity content, prove that the additives process is generally not satisfactory.

2.2.6 Pressureless sintering with amorphous carbon additions

The addition of free graphite can be made to obtain fine-grained compounds near the theoretical density.[10–12,14,39–41] The carbon addition may be better produced by in-situ pyrolysis of a Novolaque-type phenol–formaldehyde resin (≈9 wt %). The residual free carbon content is 2–2·5 wt %

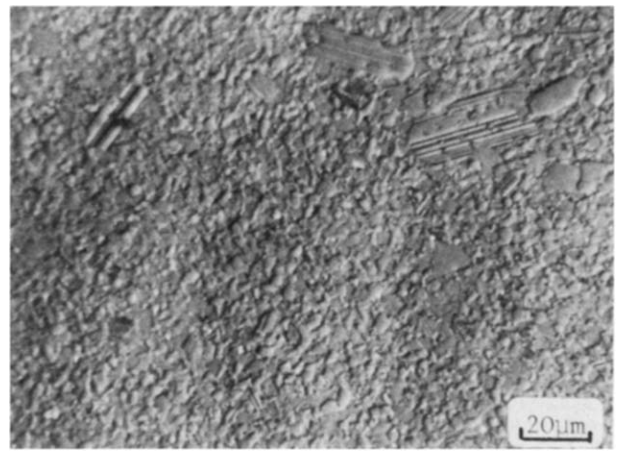

Fig. 5. Arc-melted powder, pressureless sintered with a phenol–formaldehyde resin addition; mean grain size 2 μm; some large grains are present.

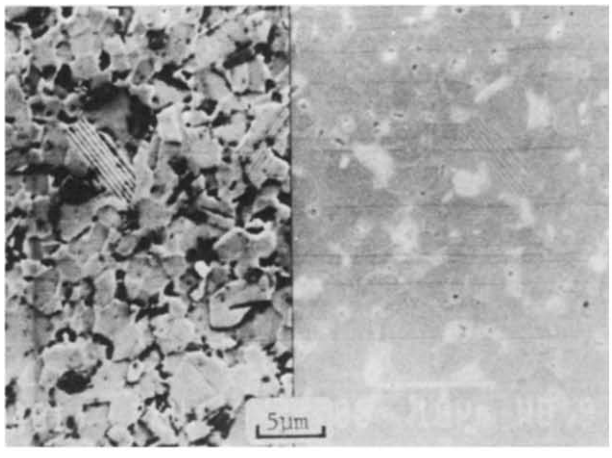

Fig. 6. Same sample as in Fig. 5, after electrolytical etching. Left: Secondary electrons; right: back-scattered electrons; the white spots are free carbon (2·5 wt.%).

(Figs 5–7).[10,11] This method is now possible in industry.[10–12,14,39–41]

A promising new method is the use of two organic precursors, e.g. polycarbosilane with a small amount of phenolic resin, giving SiC and C by in-situ pyrolysis; the resulting boron carbide ceramics have a high density (>92%) and contain no free carbon and a small amount of SiC (≈5 wt%) (Fig. 8).[10,14,42]

2.3 Laboratory preparative routes

For recent reviews see Refs 9 and 43.

2.3.1 Powders—some recent encouraging new routes

A hydrogen–Ar plasma using a BCl_3–CH_4–H_2 mixture, produces boron carbide powders in excellent yield, with a wide stoichiometry range (B/C:15·8–3·9) and a fine spherical granularity (20–30 nm).[44–46] Ultrafine (34 nm) B_4C powders are prepared by the CO_2 laser-driven pyrolysis of the same BCl_3–$CH_4(C_2H_4)H_2$ mixture. The sintering of the later powders should be promising, unfortunately they are still not commercially available.[47,48]

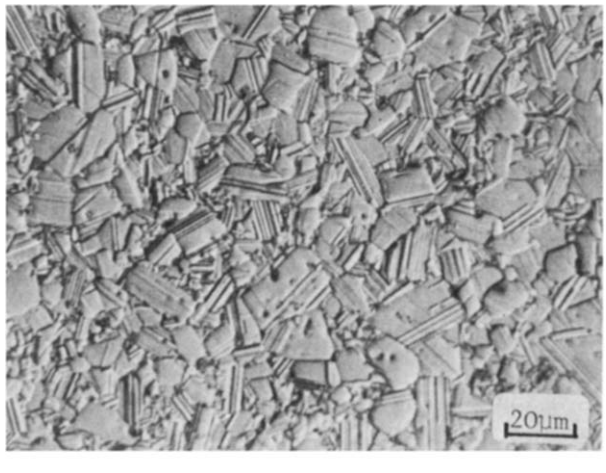

Fig. 7. Magnesiothermal powder, pressureless sintered with a phenol–formaldehyde resin addition; mean grain size 8·4 μm.

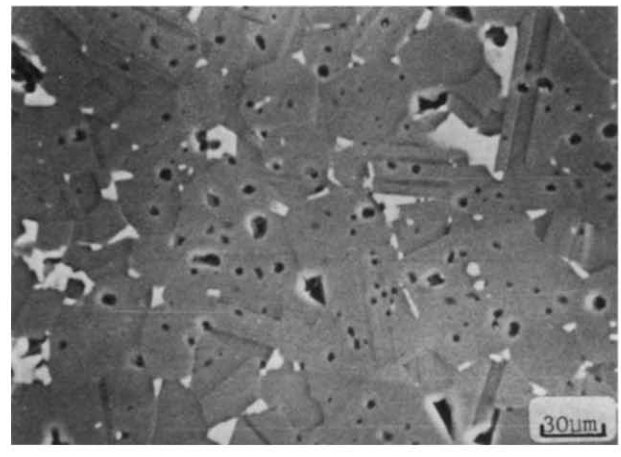

Fig. 8. SEM micrograph of an electrolytically etched sample, obtained by pressureless sintering of an arc-melted powder, with addition of polycarbosilane (7·5 wt.%) and phenolic resin (2·5 wt.%). The light phase is SiC, generally intergranular; some fine grains (<3 μm) are intragranular.

An amorphous B–C–Cl precursor precipate is obtained by reaction of CCl_4 with BCl_3 in *n*-heptane in the presence of sodium. After pyrolysis, very fine, agglomerated, irregular particules of B_4C mixed with 10% carbon excess, are obtained.[49,50]

The pyrolysis of boron-containing organic precursors may produce B_4C, pure or with BN, SiC, SiO_2, etc., generally with low yields.[51]

2.3.2 Thin solid films obtained by CVD

Films are deposited on different substrates, at high temperatures (1273–2073 K), using different reactions:

$$4BCl_3(BBr_3) + CH_4 + H_2 \rightarrow B_4C + 12HCl \quad (5)$$

$$BCl_3 + CCl_4 + 8H_2 \rightarrow B_4C + 6HCl \quad (6)$$

Calculations and models are used in order to predict the conditions and the nature of B–C deposits:[52–56] i.e. boron carbide rhombohedral-type phase, tetragonal $B_{50}C_2$, β-boron, graphite, either alone or co-deposited.[57]

The mixture BBr_3[58] (or B_2H_6[59,60])–CH_4–H_2 was studied in a microwave plasma (PACVD) at a moderate temperature (400–600°C); very hard (5000 kg/mm^2) amorphous boron–carbon films were deposited, and the maximum microhardness was obtained for 38 at. C% (outside the phase homogeneity range).[58]

2.3.3 Fibers

They are obtained by CVD of (i) boron on a carbon fiber, followed by reaction (ii) B_4C, using reaction (5),

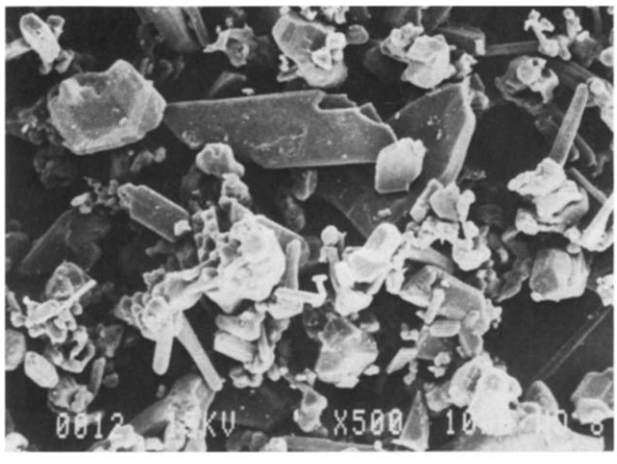

Fig. 9. (Commercial) mixture of whiskers, platelets and powder.

on a boron fiber. These fibers reinforce light metals matrices (Al, Ti, etc.).

2.3.4 Crystal growth

Single crystals are obtained using (i) CVD reactions (5), or better (6); (ii) zone melting of a boron carbide rod and (iii) metal (Cu, Pd, Pt) melts leading to the stoichiometric B_4C crystals.[61-63] Whiskers and platelets, with different stoichiometries, are prepared according to reaction (6) (Fig. 9).[64]

3 Analytical Characterization

3.1 Destructive methods for the total C and B content determination[65]

Boron carbide is totally oxidized by fusion with alkaline carbonate, the resulting product being dissolved by HCl. The total boron content is determined either by atomic absorption or emission spectroscopies or as orthoboric acid H_3BO_3, complexed by mannitol, titrated by soda using potentiometry. After oxidation by oxygen at 1600°C, the total carbon is determined as CO_2 by conductimetry or gas chromatography. Several methods are available to characterize free boron, metallic impurities.[65]

3.2 Non-destructive methods for quantitative analysis

Operating on polished dense materials, the total boron and carbon contents are determined by microanalysis. Optimum conditions for the microanalysis, as well as the choice of principal parameters (accelerating voltage, standards, back ground measurements, etc.) have been determined. The principles of the corrective method, which is especially suitable for very light elements, have been examined. The correction for carbon is very important, depending on voltage. Pure boron and diamond standards have been used. The method has been tested with a homogeneous boron carbide of known composition. The accuracy for carbon is 2–4% and 2% for boron, the balance (B + C) being in the range 100–102%.[17,66,67]

Using a generalized method of additions of graphite, it is possible to determine free graphite, present in boron carbide powders, using quantitative XRD and the ratio IC (002)/IB_xC (021).[17,67] Very fine graphite particles (0·1 μm) (so called 'subtle' carbon) could be excluded by this method.[68,69]

A new X-ray diffraction method is optimized for a quantitative analysis of both graphite and boron nitride in the presence of textured, powdered or massive, boron carbide (or boron carbide–silicon carbide composites) products.[10,70]

3.3 Auger electron spectroscopy

The shapes of B-KVV and C-KVV Auger lines observed on ion-bombardment cleaned surfaces of B_9C and B_4C were relatively insensitive to the bulk stoichiometry of the samples. This indicates that the local chemical environments surrounding B and C atoms on the surface of the ion-bombardment cleaned sample do not change appreciably in going from B_9C to B_4C. Microbeam techniques used to study a fracture surface of B_9C material reveal both C-rich (the C-VVV line was graphitic in shape) and B-rich regions.[71]

Measured by Auger electron spectroscopy, the B concentration of the surface of a B_4C single crystal, heated in the range 600–1300°C, decreased with the heating time and became a steady-state value.[72]

3.4 High-resolution imaging microstructures

High-resolution transmission electron microscopy used to examine hot-pressed boron carbide shows a high density of variable width twins.[73] The same technique was used to study the radiations effects in boron carbide.[74]

4 Phase Diagram

A lot of controversial phase diagrams have been proposed in the period 1955–1960.[17,75] Later on Elliott[76] and Kieffer *et al.*[77] assumed a wide phase homogeneity range for boron carbide (9–20 at.%C) and a eutectic between B_4C and C lies at 26 at.% C and 2400°C.[77]

In order to investigate precisely the whole phase

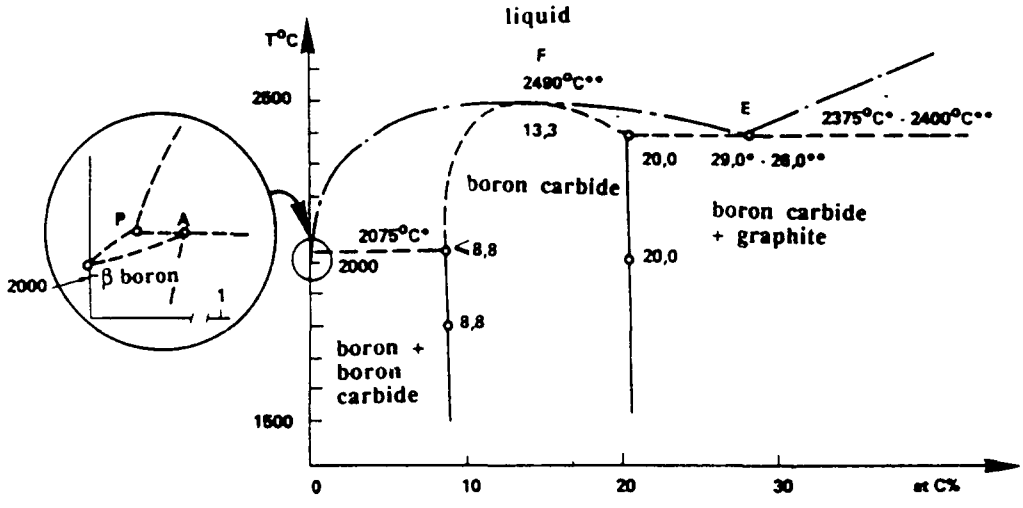

Fig. 10. Boron–carbon phase diagram. ○, Hot-pressed samples; P, peritexy; F, congruent melting; E, eutectic. *, Ref. 76; **, — —, Ref. 77; —— corresponds to 'vertical limits'; – – – –, Refs 17, 75, 78, 79.

diagram, samples prepared by melting and hot-pressing were studied. Various mixtures of β-boron and carbon powders were hot-pressed in graphite dies (1500–1800°C, 30 MPa, Ar atmosphere), then electron-beam melted under vacuum. Purification occurred during melting.[17] Crystallization proceeded from the outside to the inside, because of the thermal gradient imposed by the cooled copper crucible of the electron gun.

Samples were cut and diamond polished; their surfaces were characterized by electron microprobe analysis (cf. Section 3.2), metallographic techniques, XRD (cf. Section 5) and Knoop microhardness (cf. Section 7.5.1) measurements. The metallographic investigations, together with the microanalysis, showed that the boron carbide phase exists in the homogeneity range 9–20 at.%C (with a relative accuracy of 3–5%). In order to confirm these limits the crystal lattice dimensions (cf. Section 5) and the microhardness (cf. Section 7.5.1) of boron carbide in the above homogeneity range were studied. Boron carbide melts congruently and forms a eutectic between carbon-rich compounds and graphite. For the boron-rich compounds the existence of a peritectic transformation with a solid solution of carbon (< 1 at.%C) in the β-rhombohedral boron structure[17,75,78] was assumed.

Furthermore, samples were prepared by hot pressing (1800–2200°C, 32·5 MPa, 30–60 min, under argon) a mixture of β-boron/or carbon and boron carbide (from magnesiothermy for instance) powders. After this long soaking time, samples are considered to be in good thermodynamic equilibrium. Representing the lattice parameters variation versus C content, the breaks in the lines confirmed the same homogeneity range (8·8–20·0 at,%C, i.e. $B_{10.4}C$–B_4C)[17,79] (cf. Section 5). Therefore a phase diagram is proposed (Fig. 10).

Studying powders or hot-pressed pellets, a carbon-richer phase limit has been proposed: 21·6 at.%C ($B_{3.63}C$) at low temperature and up to 24·3 at.%C near the melting point,[80] but it has not been yet confirmed by other researchers.

CVD provides phases out of an equilibrium, with broader limits (cf. Section 2.3.2). For instance, in a deposition diagram, the rhombohedral boron carbide phase is present between at least 4 to 16 at. C%;[57] using reaction(6), single-phase crystalline materials ranging in composition from B_2C to $B_{17}C$ have been obtained.[81,82]

5 Rhombohedral Crystal Structure

The crystal structure of boron carbide has been known for a long time.[83] The lattice belongs to the $D_{3d^5} - R\bar{3}m$ space group. The rhombohedral unit cell contains 15 atoms corresponding to $B_{12}C_3$ (Fig. 11). More recent data have contested these results. Nuclear magnetic resonance (NMR) studies,[84,85] carried out on a crystal of stoichiometry close to $B_{12}C_3$, have shown that the central position in the C–C–C chain (*b* site) was partially occupied by boron (60% in Ref. 84). Using IR absorption spectroscopy Becher and Thévenot have confirmed the existence of the C–B–C chain in compounds such as B_4C and $B_{5.52}C$.[85]

The boron carbides are composed of twelve-atom icosahedral clusters which are linked by direct covalent bonds and through three-atom inter-icosahedral chains. The boron carbides are known to exist as a single phase with carbon concentrations

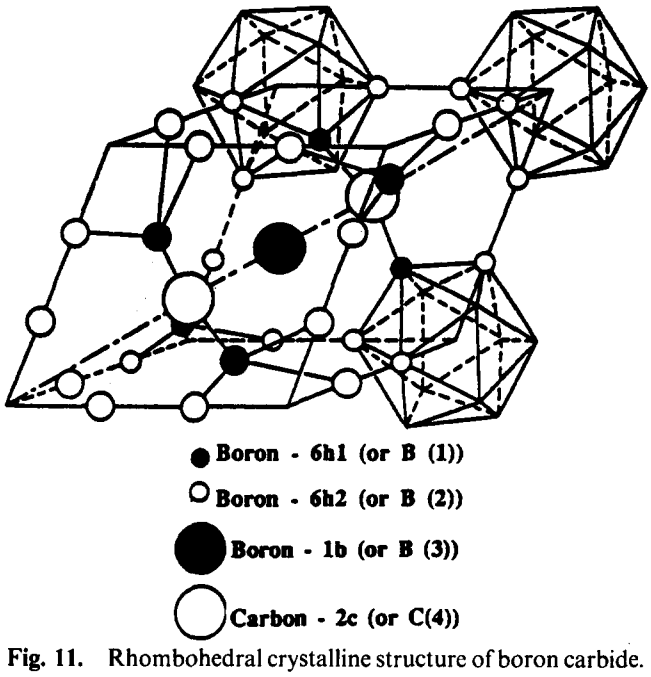

Fig. 11. Rhombohedral crystalline structure of boron carbide.

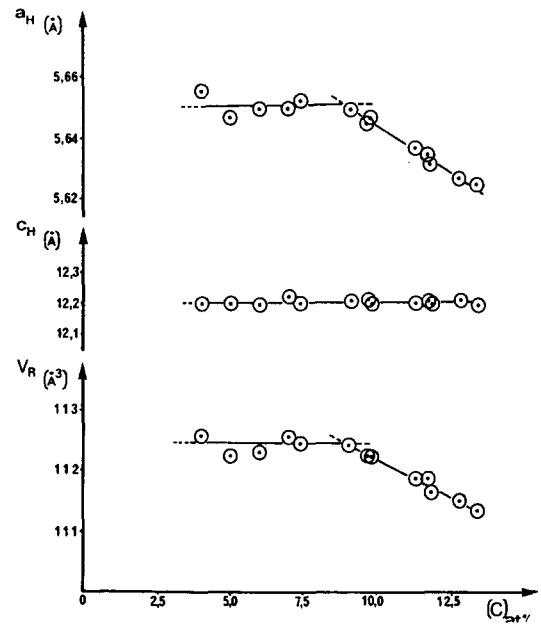

Fig. 12. Hexagonal lattice parameters and cell volume of boron-rich phases.[17,79]

from about 8·8 to 20 at.%. This range of carbon concentrations is made possible by the substitution of boron and carbon atoms for one another within both the icosahedra and intericosahedral chains[86] (Fig. 11). It is pointed out that four sites are available for a total of 15 boron and carbon atoms. The most widely accepted structural model for B_4C has $B_{11}C$ icosahedra with C–B–C intericosahedral chains.

The problem remains to know where all the boron and carbon atoms are situated exactly in the whole phase homogeneity range. Otherwise specific subunits have been proposed, i.e. B_4 chains on the boron-rich side, B_4C_2 rings, C–C–C, C–B–B chains, etc.[87] But the controversy still remains, at least partly.[87–90] It is the reason why the present authors tried to find a convenient model for the whole solid solution.[17,79,87,91]

As it has been already indicated in Section 4, the phase composition of hot-pressed boron carbide specimens containing 0–60 at.%C in a perfect thermodynamic equilibrium was studied with the help of various analytical techniques, namely chemical analysis of B and C, addition method adapted for quantitative XRD analysis, electron microprobe analysis and lattice parameter measurements.

The cell parameters a_H, c_H and the resulting volume V_R of the rhombohedral cell are represented as a function of the global composition of the samples. The straight lines, which were plotted by linear regression, intersect at a mean value of 20·1 at.%C, representing the carbon-rich composition limit and 8·8 at.%C for the boron-rich limit of the rhombohedral boron carbide phase (Figs 12 and 13). The lattice parameters of the latter two limits, of C-saturated β-rhombohedral boron and B-saturated graphite, were determined[17,79] (Tables 1 and 2).

The previous studies (lattice parameters, analysis of B and C) together with accurate measurements of the density of compounds in the phase homogeneity range allowed the determination of the number n of each atom contained in the unit cell. The value of n_T varies linearly with the carbon content, C_c:[17,91]

$$n_T = 15{\cdot}47 - 0{\cdot}019\ C_c \text{ at.\%} \quad (r = 0{\cdot}994)$$

The gradients of the plots of the parameters a_H, c_H, a_R and α_R as a function of the C content are discontinuous at the composition 13·33 at.%C ($B_{13}C_2$) (Fig. 14). This experimental result confirms the particular role of this composition within the

Table 1. Lattice parameters for the limiting compositions[17,79]

Carbon-saturated β-rhombohedral boron	*Limiting boron-rich boron carbide*	
$a_H = 10{\cdot}929$ Å	$a_H = 5{\cdot}651$ Å,	$a_R = 5{\cdot}213$ Å
$c_H = 23{\cdot}921$ Å	$c_H = 12{\cdot}196$ Å,	$\alpha = 65{\cdot}650°$
$V_H = 2\,474{\cdot}20$ Å^3	$V_H = 337{\cdot}29$ Å^3,	$V_R = 112{\cdot}43$ Å^3

H, Hexagonal lattice; R, rhombohedral lattice.

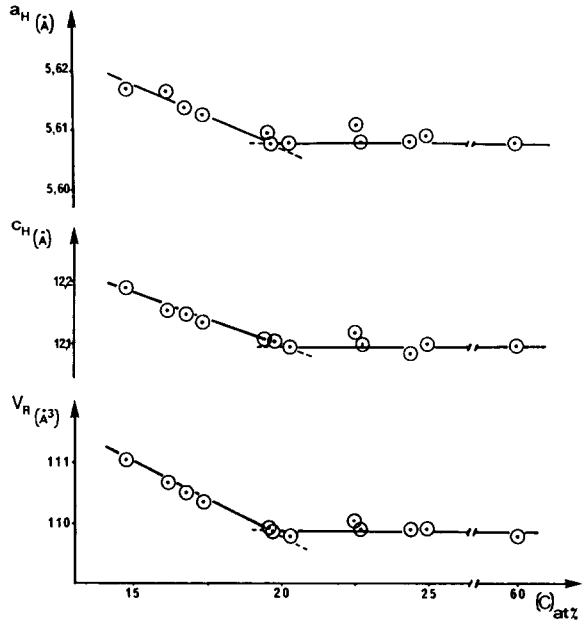

Fig. 13. Hexagonal lattice parameters and cell volume of carbon-rich phases.[17,79]

solid solution range. The volume of the rhombohedral unit cell decreases linearly with the carbon content.[17,91] A recent determination of lattice parameters of boron carbides prepared by direct synthesis between boron and carbon powders[63] shows reasonably good agreement with the work on hot-pressed samples[17,79,91] (Fig. 15). The break observed in the variation of a_H with the carbon

Table 2. Lattice parameters of carbon-rich boron carbides and of boron-saturated graphite[17,79]

Limiting Carbon-rich boron carbide		*Boron-saturated graphite*
$a_H = 5{\cdot}607$ Å	$a_R = 5{\cdot}170\,5$ Å	$a_H = 2{\cdot}470$ Å
$c_H = 12{\cdot}095$ Å	$\alpha = 65{\cdot}683°$	$c_H = 6{\cdot}739$ Å
$V_H = 329{\cdot}30$ Å^3	$V_R = 109{\cdot}77$ Å^3	$V_H = 35{\cdot}61$ Å^3

H, Hexagonal lattice; R, rhombohedral lattice.

content (Fig. 14) was not confirmed (Fig. 15). Comparing the results obtained for different preparative routes in the literature, a large scatter of the data was observed. Several explanations were proposed: (i) the composition of boron carbides is frequently not well known; (ii) small impurity concentrations can have a very large effect on the lattice parameter, and (iii) internal stresses may affect lattice parameters values.[63]

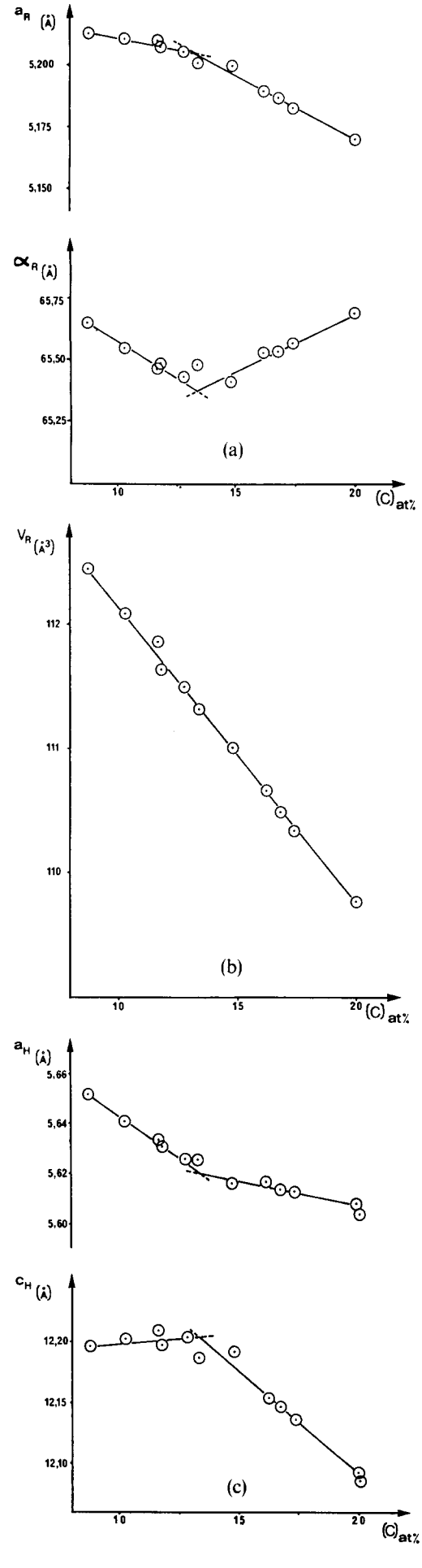

Fig. 14. (a) Rhombohedral a_R and α_R, (b) rhombohedral V_R and (c) hexagonal a_H and c_H cell parameters of boron carbide within its range of homogeneity, as a function of carbon content (measured at room temperature).[17,91]

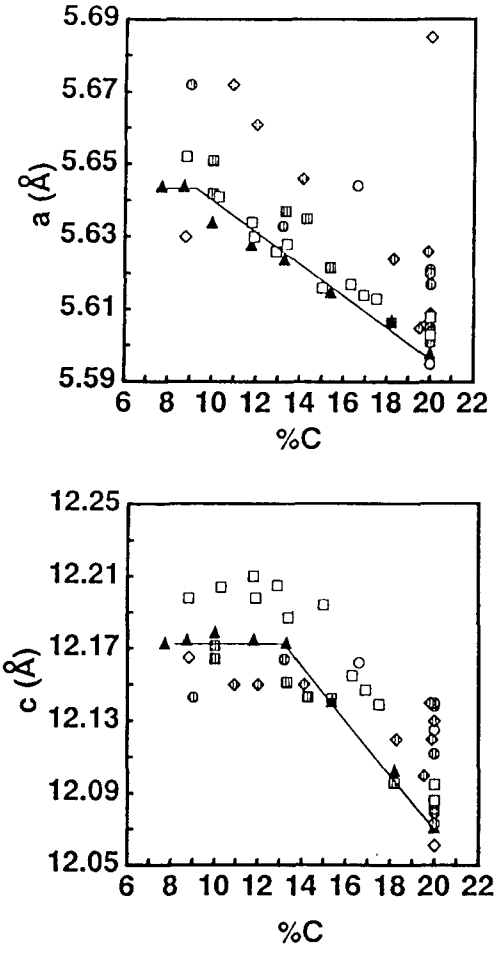

Fig. 15. Hexagonal lattice parameters of boron carbides versus composition. —▲—, Powder[63]; ▥, hot press;[63] ◍, single crystals;[92-96] □, hot press;[91] ○, CVD;[81,97] ◈, electron-beam melted,[75] and ◇, other preparations;[98,99] cited in Ref. 63.

For the carbon-rich limiting composition (20·0 at.% C) a value of 15·08 ± 0·15 atoms per unit cell, i.e. 12·06 B ± 0·08 atoms and 3·02 ± 0·08 C atoms was obtained. The lattice corresponding to the boron-rich limiting composition (8·8 at.%C) consists of 15·30 ± 0·15 atoms per unit cell, i.e. 13·95 ± 0·08 B atoms and 1·35 ± 0·08 C atoms. The unit cell corresponding to the composition 13·3 at.% C (so-called '$B_{13}C_2$') contains 15·21 ± 0·15 atoms, i.e. 13·18 ± 0·08 B atoms and 2·03 C ± 0·08 atoms.[17,91]

Finally, studies of the variation in the interatomic distances with carbon content, together with ^{13}C NMR and IR absorption spectroscopy, both characteristics of the different interatomic bonds, show the complexity of the solid solution mechanism. Two domains, separated by the 13·3 at.% C composition, have been found. In the carbon-rich compositions, up to 20 at.% C, a partial substitution of a boron atom by carbon in the B_{12} icosahedra and in the centre of the C–B–C chain is found. In the boron-rich compositions, up to 8·7 at.% C, a substitution in the C–B–C chain by boron atoms is seen. Furthermore, over the whole domain, there are interstitial atoms in the lattice (0 for 20 at.% C, 0·33 atom for 8·7 at.% C). This model appears to be the more coherent than has yet been proposed.[17,87]

$$[C] = 20\,\text{at.\%C} \rightarrow [C]13{\cdot}3\,\text{at.\%C} \rightarrow [C] = 8{\cdot}7\,\text{at.\%C}$$

$$B_{11{\cdot}77}(C_{0{\cdot}23})[C(B_{0{\cdot}23}C_{0{\cdot}77})C] \rightarrow B_{12}(CBC)B_{0{\cdot}18}C_{0{\cdot}03} \rightarrow B_{12}(CBC)_{0{\cdot}66}B_{1{\cdot}33}$$

$$n = 15 \rightarrow n = 15{\cdot}23 \rightarrow n = 15{\cdot}33$$

Considering the replacement of C atoms within B_4C, which can be written ($B_{11}C$) C–B–C, with B atoms, it was recently concluded that entropic and energetic considerations both favored this replacement within the intericosahedral chains, C–B–C → C–B–B. Once the carbon concentration is so low that the vast majority of the chains are C–B–B, near $B_{13}C_2$, subsequent substitution of C with B atoms occurs within the icosahedra, $B_{11}C \rightarrow B_{12}$. Maxima of the free energy occur at the most ordered compositions (B_4C, $B_{13}C_2$, ($B_{14}C$?)).[62,86] The evolution in the substitutions with a molecular disorder is also confirmed by Raman spectroscopy[63,100,101] and anomalous Seebeck coefficient observation.[102] X-Ray calculations indicate that the carbon atom in $B_{11}C$ icosahedra, for the B_4C stoichiometry, preferentially occupy the polar site B_2 (those connecting the icosahedra).[101,103] However, the identity of the chains have to be proved by spectroscopy and the model just considers 15 atoms, whereas the present authors have proved there are up to 15·33 atoms in the unit cell.

6 Chemical Properties[6,8]

Boron carbide is one of the most stable compounds; its standard enthalpy of formations is low (−9·3 to −17·1 kcal/mol) (−38·9 to −71·5 kJ/mol).[1] Fine powders are slowly oxidized in wet air; oxygen and water contents increase with time and species like 'B_2O_3' HBO_3 or H_3BO_3 are formed at the surface.[104]

Oxidation of hot-pressed samples in oxygen starts at 600°C and results in the formation of a thin transparent B_2O_3 film, which cracks after cooling. Up to 1200°C the oxidation process is limited by the diffusion of reagents through the oxide layer.[105-107]

Boron carbide is not attacked by cold chemical reagents; it is oxidized by hot oxidizing acids (HNO_3, H_2SO_4, $HClO_4$, etc.)[108] and fused salts (cf. Section 3.1). Chlorine attacks B_4C at 600°C, and

bromine attacks it at 800°C, giving boron trihalides; B_4C reacts with metal oxides at elevated temperatures to give carbon monoxide and metal borides.[109] Being activated by halides, B_4C is used for the boronizing of steels and alloys.[110–112] B_4C reacts with many metals that form carbides or borides at 1000°C, i.e. iron, nickel, titanium, and zirconium.[6] Aluminium and silicon form substitutional compounds with boron carbide.[6,113]

7 Physical Properties

7.1 Density[17,91]

The density of boron carbide increases linearly with carbon content within the homogeneity range of the phase according to the relationship:

$$d(\mathrm{g/cm^3}) = 2{\cdot}422_4 + 0{\cdot}0048_9[\mathrm{C}]\,\mathrm{at.\%}\ (r = 0{\cdot}998)$$

with $8{\cdot}8\,\mathrm{at.\%} \leq [\mathrm{C}] \leq 20{\cdot}0\,\mathrm{at.\%}$.

The density measured for B_4C is $2{\cdot}52\,\mathrm{g/cm^3}$; $B_{13}C_2$, $2{\cdot}488\,\mathrm{g/cm^3}$; $B_{10{\cdot}4}C$, $2{\cdot}465\,\mathrm{g/cm^{-3}}$.

7.2 Coefficient of thermal expansion (CTE)

Different determinations have been carried out:

$$\alpha = 3{\cdot}016 \times 10^{-6} + 4{\cdot}30 \times 10^{-9}t - 9{\cdot}18 \times 10^{-13}t^2 \quad (t\,^\circ C)^{114}$$

average value $\alpha = 5{\cdot}73 \times 10^{-6}\,\mathrm{K^{-1}}$ (300–1970 K)[115]

$$4{\cdot}5 \times 10^{-6}\,\mathrm{K^{-1}}\ ^{116}$$

$$4{\cdot}8 \times 10^{-6}\,\mathrm{K^{-1}}\ (25\text{–}800^\circ C)^{117}$$

The dependence of linear and anisotropic (perpendicular or parallel to c axis) CTE with temperature has been determined.[115]

7.3 Specific thermal capacity (C_p) of B_4C[118]

$$C_p\,(\mathrm{cal/mol\,K}) = 22{\cdot}99 + 5{\cdot}40 \times 10^{-3}\,T - 10{\cdot}72 \times 10^{5}\,T^{-2} \quad (T\,\mathrm{K})$$

7.4 Thermoelectrical properties

'Nuclear electric propulsion is under consideration in the USA for future outer planet missions. Previous results from a space craft system study showed that an optimum hot junction temperature is in the range of 1500 K for advanced nuclear reactor technology combined with thermoelectric conversion'[119] This is the reason why a lot of work has been carried out on that subject by SANDIA, JET Propulsion Laboratory under contract with NASA and the DOE in the USA, starting from 1981 [see Refs 120–123, for a literature review see Ref. 124].

Because there were many contradictions in the literature, mainly due to uncertain sintering routes of samples,[124] the aim of this work was to determine the dependence of the figure of merit Z [via the electrical (σ) and thermal (λ) conductivities and Seebeck coefficient (S), according to the relation $Z = S^2\sigma/\lambda$] on the temperature and carbon content within the phase homogeneity range of boron carbide. Perfectly characterized hot-pressed (Section 2.2) samples were studied.[17,124,125]

A lower than theoretical density in boron carbides reduces the thermal conductivity λ; a monotonic decline of λ with increasing temperature is noticed with B_4C; with large B/C ratios the temperature dependence is essentially nil.[17,124,126] The heat conduction mechanism occurs by phonon diffusion.[124,127] The influence of porosity and grain size on the thermal conductivity of B_4C has been studied.[127]

The electrical conductivity of boron carbides increases with temperature.[124] The conduction mechanism is explained by the small polaron hopping[128] or by a bipolaronic hopping.[129,130] The hopping activation energy E_h increases slightly when the C content increases; there is perhaps a break in the slope for 13·3 at.%C.[124]

Boron carbide is a p-type semiconductor even at very high temperature; the Seebeck coefficient S remains positive over the whole phase homogeneity range, increases slightly with temperature and reaches values of 200–300 μV/K at 1250 K. The possibility of creating efficient n-type materials remains a subject of interest; a low carbon CVD sample (90% rhombohedral phase) shows n-type behavior at room temperature.[123]

Thermal (λ) and electrical (σ) conductivities and Seebeck coefficient (S) variations versus C content exhibit a break for 13·3 at.%C; this illustrates the particular role played by this compound in the phase homogeneity range (cf. Section 5); it was not observed by other authors. For all the carbides the figure of merit Z, expressed in 1/K, increases with temperature. Furthermore for a given temperature, the 13·3 at.%C composition possesses the highest Z value, $0{\cdot}85 \times 10^{-3}$/K at 1250 K,[124] compared with $0{\cdot}5 \times 10^{-3}$/K at 1273 K obtained by Wood for B_9C.[122] The Z value obtained for the $B_{13}C_2$ compound[124] exceeds that of the best p-type Si-Ge alloys, generally used at these high temperatures;[122] this value underlines the promise of boron carbide for use in high-temperature thermoelectric generators.

7.5 Hardness and wear resistance

7.5.1 Hardness

Boron carbide is among the hardest materials (diamond, BN_c). Hardness measurements are difficult; the preparation of samples and conditions of measure are uncertain or unknown, therefore values are scattered, and difficult to be compared.[17,75,78,131] The influence of carbon content is controversial; for instance Allen[132] found an increase of hardness with C content, whereas Lipp and Schwetz did not find any influence.[131]

Therefore the conditions of Knoop microhardness (HK) determination on planar electron-gun melted samples were studied.[17,75,78,133]

Mechanical polishing induces a surface strain, therefore HK decreases when the time of electrolytic etching is increasing; HK reaches a plateau after 10 s. HK decreases when the load P increases. The variation of $\log P$ versus $\log L$ (L = length of the print), allows the determination of n in Meyer's law $P = aL^n$; after mechanical or electrolytic polishing, this variation is represented by a broken line with two slopes: i.e. (i) $n = 1{\cdot}01$ and $1{\cdot}75$ after mechanical polishing and (ii) $n = 1{\cdot}20$ and $1{\cdot}80$ after electrolytic etching.

The Knoop microhardness increases linearly with the C content in the phase homogeneity range. For instance, after mechanical polishing, $HK_{200g} = 2910 \pm 90\,kg\,mm^{-2}$ (29·1 GPa) for 10·6 at.C%, and reaches $3770 \pm 80\,kg/mm^2$ for 20 at.C% (B_4C, with the minimum volume cell (Section 5) and the maximum density (Section 7.1)). After electrolytic etching HK drops by 25%: $HK_{200g} = 2840 \pm 60\,kg/mm^2$ for B_4C.

$HK_{200} = 25{\cdot}5 \pm 2{\cdot}4$ GPa for pressureless sintered samples and $29{\cdot}0 \pm 1{\cdot}5$ for hot-pressed samples.[10,11] Values depend on microstructures, i.e. on processing and densification parameters.

Vickers hardness (HV) similarly increases with the C content in CVD samples.[134,135] Extreme hardness values were obtained by microwave plasma deposition (Section 2.3.2). There is an evolution of HV with the deposition temperature of CVD; a minimum was observed for 1373 K, which corresponds to the microstructure with a maximum grain size.[134]

Hardness decreases in the presence of free graphite in electron-beam melted,[75] sintered[11] or CVD[135] samples or Al–Si–C phase in hot-pressed boron carbide.[136]

Rebound measurements of the hardness of boron carbide indicate no decrease with temperature up to 1300°C. However, static indentation measurements show a continuous decrease of the hardness with temperature[137] (Fig. 16).

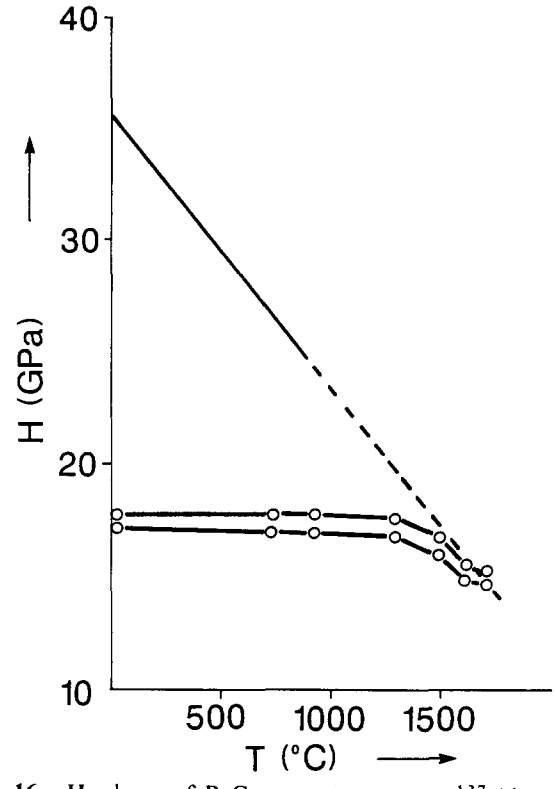

Fig. 16. Hardness of B_4C versus temperature[137] (the upper curve represents the results obtained for E (indenter) = 600 GPa, while the lower curve represents the results obtained assuming E (indenter) = 500 GPa). ———, Static indentation hardness; O——O, hardness calculated from rebound experiments.

7.5.2 Wear

Because of its high hardness and strength, boron carbide is inferior in abrasive resistance only to diamond; expressed in arbitrary units, the abrasive resistance of diamond is the top of the scale with 0·613, then boron carbide with 0·4–0·422, and silicon carbide 0·314.[8] The abrasion mechanism of B_4C was studied at 20–1400°C; plastic deformation was significant at temperatures higher than 800°C in air and vacuum; the depth of the deformation layer after reciprocal abrasion of two similar objects made of B_4C increased with the increase of the material grain size, and was 10–15 μm at 800–1000°C.[138] The friction coefficient and wear resistance of hot-pressed B_4C cylinders were studied under vacuum in the temperature range 20–1400°C; hollow cylinder face-to-face friction was carried out, under a load of 1 MPa and an average slip velocity of 0·01 m/s; the friction coefficient decreases continuously during heating from room temperature up to 1400°C, whereas the wear rate gradually increased up to 400°C, then decreases and becomes very low at 800–1000°C, and finally increases.[139,140] B_2O_3, BO(OH) and BO_3H_3 were formed on the friction interface in air.[138,139] The erosion resistance by SiC particles impact is better for B_4C than for zirconia, alumina or silicon carbide-based systems.[141]

7.5.3 Machining

Diamond tools or polishing pastes must be used. Electric spark machining is convenient and not expensive.[142,143] In particular there is no surface stress: the strength is constant with increasing etching depth.[143]

7.6 Strength

Almost all the mechanical properties measured on hot-pressed (or sintered) boron carbide samples, with close to theoretical densities, differ and depend on specific impurity contents (especially Al, Si and C used as dopants) and distribution, porosity, clusters of diffusion pores, grain size, etc. Therefore measurements are hardly comparable.[136]

Strength depends on the hot-pressing temperature and the stoichiometry of the carbide; small boron additions eliminate free graphite, thus improve strength;[16] strength would increase with the carbon content of the homogeneous carbide phase.[144] Notice that three point bending tests give higher values than four point.[105,136] Hot-pressed (σ_F = 300–500 MPa), or post-HIP treated[26] samples have higher characteristics than sintered ones (σ_F = 150–350 MPa)[10-12,14,26,39,105,136,142-144] (Table 3;[39] sintering conditions are not clearly indicated, but pressureless sintering conditions are likely to be 1900–2150°C, under reduced atmosphere (0·1 mbar), hold time 30 min (cf. Ref. 26), and hot-pressing conditions: 2100–2200°C, 20–40 MPa, under vacuum, for 15–45 min (cf. Section 2.2.1.1)).

Strength is highly variable as Weibull modulus is low (5); for all etching depths, the Weibull modulus and strength remain constant, thus the flaws are inherent to the materials.[143]

7.6.1 Influence of porosity and grain size

Transverse strength σ (compressive, or impact) decreases when porosity P, or grain size D, increase; several models have been proposed:[16,142,144]

$$\ln \sigma = 20{\cdot}337 - 0{\cdot}367 \ln D - 4{\cdot}974P$$

in which σ is in MPa, D in μm, and P is fractional porosity;[16]

$$\sigma = \sigma_0 e^{-b\omega}/\sqrt{DG}$$

where ω is the total porosity and DG the grain size.[144]

For all the stoichiometries the rupture strength decreases when the total porosity increases; it seems that the slope for a high-boron containing carbide (i.e. 80 wt% B) is higher than that for a low-boron containing carbide (i.e. 76 wt% B): therefore the influence of porosity is less important when the carbon content increases.[144] Strength decreased by a factor of 6–7, with increasing porosity from 2 to 46% and grain size from 5 to 140 μm.[142]

Fracture surface of hot-pressed boron carbide subjected to transverse rupture strength (TRS) and impact tests revealed an intercrystalline character at porosities in excess of 15%, and a mainly transcrystalline character at porosities below 15%. Rupture was of the brittle cleavage type (river patterns). There were also many twins intersected by cleavage steps.[142]

7.6.2 Behavior at high temperature

Under nitrogen atmosphere there was little or no decrease in strength[117] from its room temperature value of 380 MPa up to 1500 K (340 MPa); the fracture was fully transgranular at all testing temperatures.[143]

In air, there is a gradual decrease in strength between 600 and 1000°C, due to superficial oxidation into B_2O_3.[145] Above 1200°C, catastrophic B_4C oxidation started, which resulted in a complete degradation of strength.[105] Si and Al dopants

Table 3. Properties of hot-pressed and sintered B_4C materials[39]

Property	*Hot-pressed B_4C*	*Sintered B_4C*	
		B_4C (1 wt % C)	*B_4C (3 wt %C)*
Total carbon content[a] (wt %)	21·7	22·5	24·8
Porosity (%)	<0·5	<2	<2
Bulk density (g/cm^3)	2·51	2·44	2·46
Mean grain size (μm)	5	8	7
Flexural strength (four-point bend) (MN/m^2)	480 ± 40	351 ± 40	353 ± 30
Young's modulus (GPa)	441	390	372
Shear modulus (GPa)	188	166	158
Poisson's ratio	0·17	0·17	0·17
Fracture toughness (K_{Ic} (SENB)) (MPa m$^{1/2}$)	3·6 ± 0·3	3·3 ± 0·2	3·2 ± 0·2

[a] The amount of free carbon can be calculated approximately from $C_{free} = 1{\cdot}28\, C_{total} - 28$.

improved the oxidation resistance, thus retaining a higher strength at higher temperature (< 1400°C).[145]

7.7 Toughness (K_{Ic})

K_{Ic} is measured by indentation and SENB methods (= 2·9–3·7 MPa $m^{1/2}$).[10-12,39,105,136,143]

Using the Griffith relation for a polycrystalline dense sample, K_{Ic} was estimated to be 1·3 ± 0·3 MPa $m^{1/2}$.[144]

7.7.1 Behavior at high temperature

Under nitrogen atmosphere K_{Ic} remained constant at ≈3·7 MPa $m^{1/2}$ up to 1500 K[143] or decreased from 1·77 at 25°C to 1·31 MPa $m^{1/2}$ at 1200°C.[146]

In air, K_{Ic} is not greatly changed up to 1200°C; here, a crack propagates from a previously made notch, and a larger number of defects due to oxidation on the sample surface obviously has no influence on the K_{Ic} value.[105]

7.7.2 CVD

K_{Ic} increases with the carbon content in the phase homogeneity range (B/C: 6–4); it decreases in the presence of free graphite.[135]

7.8 Young's modulus (E)

The relationship $\nu = (E/2G) - 1$, where ν is Poisson's ratio and G the shear modulus, is given. E values are in the range 360–460 GPa.[10,11,26,39,105,136,143] E decreases slightly when temperature (up to 2000°C) and porosity P increase:[16,117,144,146,147]

$E = 460[(1 - P)/(1 + 2{\cdot}999P)]$GPa[146] and $\ln E = 26{\cdot}833 - 5{\cdot}462P$ (same expression for B_4C and boron-rich carbides).[16]

E depends on stoichiometry and decreases with the boron content.[144] Experimental values are much scattered; if specific models are considered, E can be computed, for instance $E = 498$ GPa for 84 wt% B and 418 GPa for 75 wt% B.[144]

Opposite results have been obtained recently (Table 4).[63] 'The large decrease in modulus below $B_{13}C_2$ reflects a change in the stiffness of the most compressible structural unit, the icosahedron, as $B_{11}C$ icosahedra are replaced by B_{12} icosahedra'.[63]

E is related to the composition of CVD materials (maximum value: $E = 475$ GPa for $B_{13}C_2$).[134]

Table 4. Elastic properties of boron carbide[63]

Carbon (%)	*E (GPa)*	*G (GPa)*	*ν*	*B (GPa)*
20·0	471	200	0·18	245
18·2	465	197	0·18	243
15·4	466	197	0·18	245
13·3	450	189	0·19	241
11·5	351	150	0·17	178
10·0	348	150	0·16	170
10·0	323	132	0·22	194

7.9 Poisson modulus (ν)

According to the literature, the values of ν split into two groups: 0·14 and 0·18.[143] Other values have been proposed: $\nu = 0{\cdot}17$;[39] 0·178;[143] 0·16–0·18;[26] 0·21.[147]

The variation of ν with carbon content is given in Table 4.[63]

7.10 Shear modulus (G)

G (158–188 GPa[26,39]) decreases when the carbon content decreases (Table 4).[63]

7.11 Thermal shock resistance

Experimental thermal shock resistance (determined by decrease of Young's modulus) was $\Delta T_c = 210$ K for pressureless sintered samples and 260 K for hot-pressed samples.[10,11] The maximal thermal shock resistance of B_4C pellets (used in nuclear reactors) can be predicted by $\Delta T_{c\,max} 6{\cdot}5/R$ (R is the pellet radius, in m)[127] or experimentally deduced.[117]

7.12 Fracture energy (γ_f)

Various values have been proposed: 1·6;[144] 4·5;[146] 14;[143] 18·9 J/m^2.[16] Of course, determinations were carried out on materials with different microstructures, thus with different mechanical characteristics. The general calculation of γ_f uses the Griffith relation:

$$\gamma_f = K_{Ic}^2(1 - \nu^2)/2E$$

and

$$K_{Ic} = \sigma\sqrt{CY}$$

where C is the size of the fracture-initiating flow and Y is a constant depending on the size of the specimen.

An estimate of γ using a bond energy model usually yields a good order of magnitude for covalent solids; for boron carbide it yields $\gamma = 11{\cdot}8$ J/m^2, while the calculation using Griffith relations leads to $\gamma = 14$ J/m^2.[143] 'In fracture testing, potential errors and invalid tests normally result in computed γ_f values which are greater than they should be'.[146]

Other correlations have been found. Using the Griffith criterion in the form:

$$(\sigma^2/E) = (2/\pi)(\gamma/C)$$

an approximative value of γ can be calculated from results for flexural strength and elastic modulus

using regression analysis based on the following model where D is the mean grain diameter and P the fractional porosity; the regression analysis gives the relation:[16]

$$(\sigma^2/E) = 3\,453\,801 - 751\,298 \ln D - 4\,318\,764P$$

for a definite dense microstructure, with $D = 100\,\mu m$ and $\gamma = 18{\cdot}9\,J/m^2$. This regression analysis showed that γ decreased with increasing porosity and average grain size.[16]

Other regression relations (including B content and open and closed porosity as additional variables) were also analyzed, but these additional variables did not have a significant effect on the γ value.[16]

The dependence of γ on temperature has been calculated.[143] The fracture energy at 500°C appeared to be experimentally independent of porosity.[146] For a given porosity (i.e. 8%), γ decreases when the temperature increases.[143,146]

More details and interesting discussions on γ determinations are given in Refs 143 and 146.

8 Main Industrial Applications

Details may be found in diverse reviews.[3-8] According to the previously described properties, the applications may be divided as follows.

8.1 Uses based on hardness

The major industrial use of boron carbide is as abrasive grit or powder. Particle sizes are available from 1 μm to 10 mm, used as polishing, lapping and grinding media for hard materials such as cemented carbides, technical ceramics, etc. Boron carbide is far less expensive than diamond.

A second category is wear-resistance components made of hot-pressed sintered pieces. Boron carbide sand-blasting nozzles are characterized by minimum wear, even with silicon carbide or corundum grit. Post-HIP sintered components have the best wear resistance.[26,148] Boron carbide ceramic nozzles are used for water-jet cutting.

Other wear applications include sintered B_4C wheel dressing sticks to produce new cutting edges, and mortars and pestles.

Lightweight armor plates have been used for the protection of helicopters, or as breastplates for the protection of personnel against piercing bullets.[149]

8.2 Chemical uses (cf. Section 6)

Boron carbide powders, activated by fluorides (or other halides), are used to diffuse boron at the surface of steels; the resulting Fe_2B thin layer (10–200 μm) is very hard (HV (1N) = 24 GPa) and wear resistant.[110,150] In certain cases, the formation of a brittle two-phase iron boride (FeB–Fe_2B) layer, is inconvenient; the aim is to produce a single Fe_2B phase.[111,112]

8.3 Electrical application (cf. Section 7·4)—boron carbide/graphite thermocouple

The thermocouple consists of a graphite tube, a B_4C bar, and a BN sleeve between them. It can be used to 2200°C, under inert gas or vacuum atmosphere; there is a linear relationship between its voltage and the temperature at 600–2200°C.[151-153]

8.4 Nuclear applications[4,114,154-156]

8.4.1 Principles

The main part (95%) of nuclear power is now produced in reactors controlled by two kinds of absorbing materials: boron carbide ('B_4C') or a ternary alloy (Ag–In–Cd). Boron carbide is a neutron absorber widely used because of its high B content, its good chemical inertness and high refractoriness. The neutronic absorption of B_4C is due to ^{10}B, which participates according to the following capture reaction:

$$^{10}_{5}B + {}^{1}_{0}n \rightarrow {}^{4}_{2}He + {}^{7}_{3}Li + 2{\cdot}4\,MeV$$

The cross-section of this reaction varies from 3850 barns for thermal neutrons to a few barns for fast neutrons (the law following $1/\sqrt{E}$, E = energy of neutrons), and allows the use of boron carbide with the natural isotopic content (19·8% of ^{10}B—the rest being ^{11}B) or enriched up to 90 at.% ^{10}B for reactor guiding. The absorbent nuclear material depends on the specific reactor.

8.4.2 The main present reactors[155,156]

Pressurized water reactors (PWR) are the most widely used in the world, and used by Electricité de France (EDF) in France. Two kinds of reactors now exist: 900 MW, where the Ag–In–Cd alloy only is used, and the last generation 1300 MW in which B_4C is partly substituted for the alloy.

Fast breeder reactors (FBR), more recent than PWR, their standardization is not completely achieved, but boron carbide is now recognized as a neutron absorber. In fact ^{10}B is one of the nuclides which reveals the best behavior under fast neutrons: a large cross-section (1 barn in a standard spectrum of a 0·7 MeV average energy) and no resonance in the whole spectrum.

According to the design of the reactor core (number of barns), 'natural' boron (19·8% ^{10}B) or

enriched is used: on the one hand, 48% for Phenix, and on the other hand 90% in Rapsodie (stopped in 1983) or Superphenix. Enrichment (obtained by chemical exchange reactions, or by using resins) is a tedious and very expensive route: the price of 1 g carbide with 90% ^{10}B is near 4–5 ECUS (or US dollars), whereas 'natural' boron carbide costs 15–75 ECUS/kg.[6]

8.4.3 Control rods in PWR[157]

'The fissile material (U_{235}) is placed inside the reactor core in the form of fuel assemblies. These assemblies measure from 4 to 4·8 m in length... Each fuel assembly consists of 264 zirconium tubes or rods, which contain uranium dioxide fuel pellets. The rods are secured in a square framework or 'skeleton' by means of 8 to 10 grids, two nozzles and 24 guide thimbles. The control rods slide inside the guide thimbles to conduct the rate of nuclear reaction'.[157] The rod cluster control assembly is constituted by 24 stainless steel cylinders, 4 m in length, in which calibrated boron carbide pellets (diameter 7–8 mm, height 15 mm, weight $\approx$ 1·4 g) are piled, under argon atmosphere.

8.4.4 Fabrication of boron carbide pellets

Boron carbide powders are sintered (cf. Section 2.2).

As an absorber for PWR 'natural' boron carbide (19·8% ^{10}B) is used; pellets are pressureless sintered, the density is $\approx$ 70% d_{th}. In France, the Compagnie Franco Belge de Fabrication de Combustibles (FBFC) produces 2000 m of pellets per year, i.e. $\approx$ 190 kg, corresponding to one reactor core.

Boron carbide is also used as an absorber for FBR (Superphenix and Phenix). The diameter of pellets is 20 mm in the main control system, and 45 mm in the complementary system. Pellets are hot-pressed to reach 96% d_{th}.

8.4.5 Behavior under neutron irradiation

The degree of irradiation of boron carbide is expressed either by a relative value (ratio of consumed ^{10}B atoms to initial number of total atoms) or an absolute value by the capture density (number of consumed ^{10}B atoms—equivalent to the number of He or Li, appeared during irradiation—pro volume unit). The lifetime of boron carbide in the control rod does not reach the theoretical limit fixed by the total consumption of ^{10}B, because of the destruction of the material due to the large volume of He produced. For an irradiation corresponding to 10^{22} captures/cm^3 of B_4C (typical value in FBR for a 330-day period), 0·12 g of lithium and 380 cm^3 helium are produced in a 1 cm^3 absorber. Under the temperature influence, a part (50–90%) of the helium diffuses outside the material, whereas a part accumulates, thus producing swelling and microcracking, which can break up a pellet into a fine powder. These processes are rather insensitive to the irradiation parameters (temperature, flux and neutron spectrum).[74] The combination of swelling (increase of 15 vol% for 10^{22} captures/cm^3) and the desegregation of the material induces, for heavy irradiations ($> 10^{22}$ captures/cm^3), a strong mechanical interaction between the absorber and the stainless steel tube, which may be broken. This tube is also fragilized under fast neutrons irradiation and by diffusion of both boron and carbon (especially free) coming from the absorber itself; in Superphenix, boron carbide is directly cooled by metallic sodium, inside the steel tube.

The mean lifetime of an absorber in a PWR is 15 years, whereas it should be one year in the fast breeder, for a maximum density of captures respectively of 0·5 10^{22}/cm^3 and 1·2 10^{22}/cm^3.

Samples irradiated by the fast neutrons of a reactor were studied by transmission electron microscopy in order to understand the respective roles of helium and point defects in relation with swelling and microcracking.[74]

9 Conclusion

Actually, boron carbide is a fascinating technical ceramic.

Annual production in the non-Communist countries is about 500 t, which is rather small compared to the 500 000 tonnes SiC production.[6]

Among the industrial uses, nuclear applications are the most valuable and promising. The price of ^{10}B-enriched boron carbide is very high (cf. Section 8.4.2) but the development of fast neutron reactors needs boron carbide. Problems due to swelling under irradiation remain, and they have to be solved. Research is being carried out, for instance in France.

Powders are usually prepared either by magnesiothermy or arc melting. Perhaps new reactive powders, from plasma or laser techniques, could be interesting for low temperature pressureless sintering. Organic boron precursors are not yet developed, but should be useful as sintering additives.[43]

New forms such as platelets and whiskers for boron carbide are just appearing (cf. Section 2.3.4).[64]

Several composite systems are now studied: cermets with Al;[158–160] composites B_4C–C and B_4C–SiC;[10,14,161,162] B_4C–SiC whiskers;[163]

B_4C–TiB_2.[116] Specific applications for the latter are still to be developed.

Acknowledgements

Thanks are due to M. Wache (FBFC, Romans, France), B. Kryger (CEN Saclay), G. Ossena (Cogema, France), for information on nuclear applications, K. A. Schwetz (ESK, FRG) and the firm Quartz & Silice (Nemours, France) for other industrial applications.

The author appreciates the valuable contributions of former students M. Bouchacourt[17] and M. Bougoin[10] to the increase of knowledge about boron carbide, and does not forget the care of M. C. Mathais in typing the manuscript.

References

1. Thévenot, F. & Bouchacourt, M., Le carbure de bore: matériau industriel performant, 1 ère partie: le point des connaissances physico-chimiques. *Ind. céramique*, **732** (1979) 655–61.
2. Rigdway, R. R., Boron carbide. A new crystalline abrasive and wear-resisting product. *Trans. Am. Electrochem. Soc.*, **66** (1934) 117–33.
3. Lipp, A., Boron carbide. Production, properties, application. *Techn. Rundschau*, **14**, **28**, **33** (1965); **7** (1966).
4. Beauvy, M. & Thévenot, F., Le carbure de bore: matériau industriel performant. 2ème partie: applications industrielles du carbure de bore. *Ind. céramique*, **734** (1979) 811–14.
5. Schwetz, K. A., Reinmuth, K. & Lipp, A., Herstellung und industrielle Anwendung refraktäre Borverbindungen. *Radex Rundschau*, **3** (1981) 568–85.
6. Schwetz, K. A. & Lipp, A., Boron carbide, boron nitride, and metal borides. *Ullmann's Encycl. Indust. Chem.*, **A4** (1985) 295–307.
7. Thévenot, F., Quelques applications actuelles des borures. *Silicates Industriels*, **51** (1986) 17–22.
8. Makarenko, G. N., Borides of the IVb group. In *Boron and Refractory Borides*, ed. V. I. Matkovich. Springer Verlag, Berlin, 1977, pp. 310–30.
9. Thévenot, F., Formation of carbon–boron bonds. In *Inorganic Reactions and Methods*, Vol. 10, ed. J. J. Zuckerman & A. P. Hagen, VCH Publishers, New York, 1989, pp. 2–11.
10. Bougoin, M., Frittage sans charge du carbure de bore et de composites carbure de bore–carbure de silicium. Propriétés mécaniques. Thesis, Ecole des Mines de Saint-Etienne, France, 1985.
11. Bougoin, M., Thévenot, F., Dubois, J. & Fantozzi, G., Synthèse et caractérisation de céramiques denses en carbure de bore. *J. Less Common. Met.*, **114** (1985) 257–71.
12. Thévenot, F. & Bougoin, M., Pressureless sintering of boron carbide phase. In *Boron-Rich Solids, AIP Conf. Proc. 140*, ed. D. Emin, T. Aselage, C. L. Beckel, I. A. Howard & C. Wood. Amer. Inst. Phys., New York, 1986, pp. 51–8.
13. Gray, E. G., Boron carbide. *European Patent Application*, 1152428, May 1980; Application 1978.
14. Thévenot, F., Sintering of boron carbide and boron carbide–silicon carbide two-phase materials and their properties. *J. Nucl. Mater.*, **152** (1988) 154–62.
15. Angers, R. & Beauvy, M., Hot pressing of boron carbide. *Ceram. Int.*, **10** (1984) 49–55.
16. Champagne, B. & Angers, R., Mechanical properties of hot-pressed B–B_4C materials. *J. Am. Ceram. Soc.*, **62** (1979) 149–53.
17. Bouchacourt, M., Etudes sur la phase carbure de bore—corrélations propriétés–composition. Thèse d'état, INPG, Ecole des Mines de Saint-Etienne, France, 1982.
18. Bouchacourt, M., Brodhag, C. & Thévenot, F., The hot pressing of boron and boron rich compounds: B_6O, $B_{10.5}C$–B_4C. *Sci. Ceram.*, **11** (1981) 231–6.
19. Brodhag, C., Bouchacourt, M. & Thévenot, F., La cinétique de compression à chaud de céramiques spéciales. *Silicates Industriels*, **45** (1981) 91–101.
20. Brodhag, C., Bouchacourt, M. & Thévenot, F., Comparison of the hot pressing kinetics of boron, boron suboxide B_6O and boron carbides. In *Materials Science Monographs, 16, Ceramic powders*, ed. P. Vincenzini. Elsevier, Amsterdam, 1983, pp. 881–90.
21. Telle, R. & Petzow, G., Reaction sintering of boron carbide (B_4C) with silicon and titanium. *Horiz. Powd. Metall., Proc. Int. Powd. Metall. Conf. Exhib.*, **2** (1986) 1155–8.
22. Telle, R. & Petzow, G., Mechanisms in the liquid-phase sintering of boron carbide with silicon based melts. *Mater. Sci. Monogr.*, **38A** (1987) 961–73.
23. Larker, H. T., Hermansson, L. & Adlerborn, J., Hot isostatic pressing and its applicability to silicon carbide and boron carbide. *Mater. Sci. Monogr.* **38A** (1987) 795–803.
24. Alderborn, J., Isaksson, S. & Larker, H., Hot-pressing of parts from boride, carbide, or nitride powders. *Ger. Pat.*, 2344648, 1974.
25. ASEA, Manufacture of boron carbide articles. Japanese Patent 62207762, 1987.
26. Schwetz, K. A., Grellner, W. & Lipp, A., Mechanical properties of HIP-treated sintered boron carbide. *Inst. Phys. Conf.*, Series No. 75, 1986, Chapter 5, pp. 413–26.
27. Holcombe, C. E., New microwave coupler material. *Ceram. Bull.*, **62** (1983) 1388.
28. Katz, J. D., Blake, R. D., Petrovic, J. J. & Sheinberg, H., Microwave sintering of boron carbide. *Met. Powd. Rep.*, **43** (1988) 835–7.
29. Prümmer, R., Explosive Werkstoffbearbeitung. *Keram. Z.*, **37** (1985) 243–5.
30. Bairamashvili, I. A., Kalandadze, G. I., Dzhobava, D. S. & Eristavi, A. M., Sintering of boron carbide powders after static and explosive treatment. *Soobshch. Akad. Nauk. Gruz. SSR*, **119** (1985) 161–3.
31. Grabchuk, B. L. & Kislyi, P. S., Sintering of boron carbide. *Porosh. Met.*, **8** (1974) 11–16.
32. Kuzenkova, M. A., Kislyi, P. S., Grabchuk, B. L. & Bodnaruk, N. I., The structure and properties of sintered boron carbide, *J. Less Common Met.*, **67** (1979) 217–23.
33. Kuzenkova, M. A., Kislyi, P. S., Grabchuk, B. L. & Bodnaruk, N. I., The structure and properties of sintered boron carbide. *Powd. Met. Int.*, **12** (1986) 11–13.

34. Grabchuk, B. L. & Kislyi, P. S., Sintering of technical boron carbide. *Porosh. Met.*, **7** (1975) 27–31.
35. Weaver, G. Q., Sintered high-density boron carbide. US Patent, 4 320 204, 1982.
36. Zakhariev, Z. & Radev, D., Properties of polycrystalline boron carbide sintered in the presence of tungsten boride (W_2B_5) without pressing. *J. Mater. Sci. Lett.*, **7** (1988) 695–6.
37. Oh, J. H., Orr, K. K., Lee, C. K., Kim, D. K., Lee, J. K. & Kim, C. H., Sintering of boron carbide. *J. Korean Ceram. Soc.*, **22** (1985) 60–6.
38. Kanno, Y., Kawase, K. & Nakano, K., Additive effect on sintering of boron carbide. *J. Ceram. Soc. Jap.*, **95** (1987) 1137–40.
39. Schwetz, K. A. & Grellner, W., The influence of carbon on the microstructure and mechanical properties of sintered boron carbide. *J. Less Common Met.*, **82** (1981) 37–47.
40. Prochazska, S., Dole, S. L. & Hejna, C. I., Abnormal grain growth and microcracking in boron carbide. *J. Am. Ceram. Soc.*, **68** (1985) C-235-6.
41. Dole, S. L. & Prochazska, S., Densification and microstructure development in boron carbide. *Ceram. Eng. Sci. Proc.*, **6** (1985) 1151–60.
42. Bougoin, M. & Thévenot, F., Pressureless sintering of boron carbide with an addition of polycarbosilane. *J. Mater. Sci.*, **22** (1987) 109–14.
43. Thévenot, F., Laboratory methods for the preparation of boron carbides. In *NATO Adv. Res. Workshop (ARW), The Physics and Chemistry of Carbides, Nitrides and Borides*, ed. R. Freer. Manchester, UK, September 1989. Kluwer Academic Publ., NATO ASi Series, Dordrecht, 1990, pp. 87–96.
44. MacKinnon, I. M. & Wickens, A. J., The preparation of boron carbide using a radio frequency plasma. *Chem. Ind. (London)*, 1973, 800.
45. MacKinnon, I. M. & Reuben, B. G., The synthesis of boron carbide in a r.f. plasma. *J. Electrochem. Soc.*, **122** (1975) 806–11.
46. MacKinnon, I. M., Hamblyn, S. M. L. & Reuben, B. G., Mechanism of formation of boron and boron carbide by reduction of boron trichloride in an r.f. plasma. *I.C.P. Inf. Newslett.*, **3** (1977) 311–12.
47. Knudsen, A. K. & Langhoff, C. A., Submicron-sized boron carbide powders. PCT Application, WO 86 04 524, 1986; US Application 1985.
48. Knudsen, A. K., Laser-driven synthesis and densification of ultrafine boron carbide powders. *Adv. Ceram.*, **21** (1987) 237–47.
49. Ritter, J. J., A low temperature chemical process for precursors to boride and carbide ceramic powders. *Adv. Ceram.*, **21** (1987) 21–31.
50. Ritter, J. J., Refractory borides and carbides. US Patent 4 606 902, 1986.
51. Walker, Jr., B. E., Rice, R. W., Becher, P. F., Bender, B. A. & Coblenz, W. S., Preparation and properties of monolithic and composite ceramics produced by polymer pyrolysis. *Ceram. Bull.*, **62** (1983) 916–23.
52. Bernard, C., Deniel, Y., Jacquot, A., Vay, P. & Ducarroir, M., Détermination des équilibres chimiques complexes dans les systèmes polyphasés. I. Méthode de traitement. *J. Less Common Met.*, **40** (1975) 165–71.
53. Ducarroir, M. & Bernard, C., Thermodynamic domains of the various solid deposits in the B–C–H–Cl vapor system. In *Proc. Chemical Vapor Deposition Fifth Intern. Conf.*, 1975, pp. 72–83.
54. Ducarroir, M. & Bernard, C., Thermodynamic domains of the various solid deposits in the B–C–H–Cl vapor system. *J. Electrochem. Soc.* **123** (1976) 136–40.
55. Vandenbulcke, L., Theoretical and experimental studies on the chemical vapor deposition of boron carbide. *Ind. Eng. Chem. Prod. Res. Dev.*, **24** (1985) 568–75.
56. Rebenne, H. & Pollard, R., Theoretical analysis of chemical vapor deposition of ceramics in an impinging jet reactor. *J. Am. Ceram. Soc.*, **70** (1987) 907–18.
57. Lartigue, S. & Male, G., Contribution to the study of tetragonal compounds in the boron carbon system. *J. Mater. Sci. Lett.*, **7** (1988) 153–6.
58. Cholet, V., Herbin, P. & Vandenbulcke, L., CVD of boron carbide from BBr_3–CH_4–H_2 mixtures into a microwave plasma. In *Proc. 9th Int. Symp. Boron, Borides and Related Compounds*, Duisburg, FRG, September 1987, pp. 423–4.
59. Veprek, S. & Jurcik-Rajman, M., Plasma-induced deposition of amorphous boron carbide. In *Symp. Proc. 7th Int. Symp. Plasma Chem.*, 1985, pp. 90–4.
60. Toyoda, H., Sugai, H., Isozumi, T. & Okuda, T., Formation of pure boron and boron–carbon alloys by a toroidal glow discharge. In *Proc. 9th Int. Symp. Boron, Borides and Related Compounds*, Duisburg, FRG, September 1987, pp. 409–10.
61. Aselage, T. L., Preparation of boron-rich refractory semiconductors. In *Novel Refractory Semiconductors*, ed. D. Emin, T. L. Aselage & C. Wood. MRS, Pittsburg, Pennsylvania, 1987, pp. 101–11.
62. Aselage, T. L., Van Deusen, S. B. & Morosin, B., Solution growth, composition, and structure of boron carbide crystals. *J. Less. Common Met.*, to be pub.
63. Aselage, T. L., Tallant, D. R. and Gieske, J. H., Preparation and properties of icosahedral borides. In *NATO Adv. Res. Workshop (ARW), The Physics and Chemistry of Carbides, Nitrides and Borides*, Manchester, UK, September 1989. Kluwer Academic Publ., NATO ASi Series, Dordrecht, 1990, pp. 97–111.
64. Weaver, S. C., Nixdorf, R. D. & Vaughan, G., SiC whiskers and platelets. In *Ceramic Transactions, Silicon Carbide 87*, Vol. 2, ed. J. D. Cawley & C. E. Semler. Am. Ceram. Soc., Westerville, Ohio, 1989, pp. 397–406.
65. Thévenot, F. & Cueilleron, J., Analytical problems in boron and refractory borides. *Analysis*, **5** (1977) 105–21.
66. Ruste, J., Bouchacourt, M. & Thévenot, F., Etudes sur le carbure de bore. II. Microanalyse électronique quantitative. *J. Less Common Met.*, **59** (1978) 131–8.
67. Bouchacourt, M., Thévenot, F. & Ruste, J., Analyses par microsonde électronique et méthodes chimiques destructrices appliquées à l'étude du système bore–carbone. *J. Microsc. Spectros. Electron.*, **4** (1979) 143–6.
68. Zuppiroli, L., Kormann, R. & Lesueur, D., Etude fondamentale sur le carbure de bore. CEA-R-5237, Centre d'Etudes Atomiques, CEN, Saclay, France, 1983.
69. Bandyopadhyay, A. K., Beuneu, F., Zuppiroli, L. & Beauvy, M., The role of free carbon in the transport and magnetic properties of boron carbide. *J. Phys. Chem. Sol.*, **45** (1984) 207–14.
70. Bougoin, M., Fillit, R., Thévenot, F. & Bruyas, H., Determination of free graphite in textured samples of boron carbide and boron carbide–silicon carbide composites. *J. Less Common Met.*, **117** (1986) 215–23.

71. Madden, H. H., Nelson, G. C. & Wallace, W. O., Auger electron spectroscopy studies of boron carbide. In *Boron-Rich Solids, AIP Conf. Proc. 140*, ed. D. Emin, T. Aselage, C. L. Beckel, I. A. Howard & C. Wood. Amer. Inst. Phys., New York, 1986, pp. 121–9.
72. Iuoue, S., Fukuda, S., Hino, T. & Yamashina, T., Change of surface composition of boron carbide (B_4C) single crystal due to heat treatment. *J. Vac. Sci. Technol. A*, **5** (1987) 1279–82.
73. MacKinnon, I. D. R., Aselage, T. & Van Deusen, S. B., High-resolution imaging of boron carbide microstructures. In *Boron-Rich. Solids, AIP Conf. Proc. 140*, ed. D. Emin, T. Aselage, C. L. Beckel, I. A. Howard & C. Wood. Amer. Inst. Phys., New York, 1986, pp. 114–20.
74. Stotto, T., Etude par microscopie électronique des effets d'irradiation dans le carbure de bore. Thesis, Université Paris Sud, 1986; CEA-R-5382, Centre d'Etudes Atomiques, CEN Saclay, France, 1987.
75. Bouchacourt, M. & Thévenot, F., Etudes sur le carbure de bore. III. Domaine d'existence de la phase carbure de bore. *J. Less Common Met.*, **59** (1978) 139–52.
76. Elliott, R. P., The boron carbon system, Contract No. AT (11-1), 578, Project Agreement No. 4, Armour Res. Found, Rep. ARF 220012 (Final Tech. Rep.), 7 June 1961.
77. Kieffer, R., Gugel, E., Leimer, G. & Ettmayer, P., Untersuchungen zum System Bor–Kohlenstoff. *Ber. DKG*, **48** (1971) 385–9.
78. Bouchacourt, M. & Thévenot, F., The melting of boron carbide and the homogeneity range of the boron carbide phase. *J. Less Common Met.*, **67** (1979) 327–31.
79. Bouchacourt, M. & Thévenot, F., Analytical investigations in the B–C system. *J. Less Common Met.*, **82** (1981) 219–26.
80. Beauvy, M., Stoichiometric limits of carbon-rich boron carbide phases. *J. Less Common Met.*, **90** (1983) 169–75.
81. Kevill, D. N., Rissmann, T. J., Brewe, D. & Wood, C., Growth of crystals of several boron–carbon compositions by chemical vapor deposition. *J. Cryst. Growth*, **74** (1986) 210–16.
82. Kevill, D. N., Rissmann, T. J., Brewe, D. & Wood, C., Preparation of boron–carbon compounds, including crystalline B_2C material by chemical vapor deposition. *J. Less Common Met.*, **117** (1986) 421–5.
83. Clark, H. K. & Hoard, J. L., The crystal structure of boron carbide. *J. Am. Chem. Soc.*, **65** (1943) 2115–19.
84. Silver, A. H. & Bray, P. J., Nuclear magnetic resonance of boron carbide. *J. Chem. Phys.*, **31** (1959) 247–53.
85. Becher, H. J. & Thévenot, F., Infrarotspektroskopische Untersuchung des Borcarbids und seiner isotypen Derivate $B_{12}O_2$, $B_{12}P_2$ und $B_{12}As_2$. *Z. Anorg. Allg. Chem.*, **410** (1974) 274–86.
86. Emin, D., Structure and single-phase regime in boron carbides. *Phys. Rev. B*, **38** (1988) 6041–55.
87. Conard, J., Bouchacourt, M., Thévenot, F. & Hermann, G., ^{13}C and ^{11}B NMR investigations in the boron carbide phase homogeneity range: a model of solid solution. *J. Less Common Met.*, **117** (1986) 51–60.
88. Bray, R. J., NMR studies of borates and borides. In *Boron-Rich Solids, AIP Conf. Proc. 140*, ed. D. Emin, T. Aselage, C. L. Beckel, I. A. Howard & C. Wood. Amer. Inst. Phys., New York, 1986, pp. 142–67.
89. Alexander, M. N., NMR studies of the structure of boron carbides. In *Boron-Rich Solids, AIP Conf. Proc. 140*, ed. D. Emin, T. Aselage, C. L. Beckel, I. A. Howard & C. Wood. Amer. Inst. Phys., New York, 1986, pp. 168–76.
90. Duncan, T. M., The distribution of carbon in boron carbides: ^{13}C NMR studies. In *Boron-Rich Solids, AIP Conf. Proc. 140*, ed. D. Emin, T. Aselage, C. L. Beckel, I. A. Howard & C. Wood. Amer. Inst. Phys., New York, 1986, pp. 177–88.
91. Bouchacourt, M. & Thévenot, F., The properties and structure of the boron carbide phase. *J. Less Common Met.*, **82** (1981) 227–35.
92. Morosin, B., Mullendore, A., Emin, D. & Slack, G., Rhombohedral crystal structure of compounds containing boron-rich icosahedra. In *Boron-Rich Solids, AIP Conf. Proc. 140*, ed. D. Emin, T. Aselage, C. L. Beckel, I. A. Howard & C. Wood. Amer. Inst. Phys., New York, 1986, pp. 70–86; cited in Ref. 63.
93. Morosin, B., Aselage, T. & Feigelson, R., In *Novel Refractory Semiconductors*, ed. D. Emin, T. L. Aselage & C. Wood. MRS; Pittsburg, Pennsylvania, 1987, pp. 145–50; cited in Ref. 63.
94. Will, G. & Kossobutski, K. H. An X-ray diffraction analysis of $B_{13}C_2$. *J. Less Common Met.*, **47** (1976) 43–8; cited in Ref. 63.
95. Yakel, H., Crystal structure of a boron-rich carbide. *Acta Cryst.*, **B31** (1975) 1797–1806; cited in Ref. 63.
96. Clarke, H. K. & Hoard, J. L., The crystal structure of boron carbide. *J. Am. Chem. Soc.*, **65** (1943) 2115–19; cited in Ref. 63.
97. Mierzejewski, S. & Niemyski, T., Preparation of crystalline boron carbide by vapour phase reaction. *J. Less Common Met.*, **8** (1965) 368–74; cited in Ref. 63.
98. Matkovich, V. I., Extension of the boron–carbon homogeneity range. *J. Less Common Met.*, **47** (1976) 39–42; cited in Ref. 63.
99. Sugaya, T. & Watanabe, O., Morphology of boron carbide single crystals. *J. Less Common Met.*, **26** (1972) 25–31; cited in Ref. 63.
100. Tallant, D. R., Aselage, T. L., Campbell, A. N. & Emin, D., Boron carbides: evidence for molecular level disorder. *J. Non-Cryst. Solids*, **106** (1988) 370–3.
101. Tallant, D. R., Aselage, T. L., Campbell, A. N. & Emin, D., Boron carbide structure by Raman spectroscopy. *Phys. Rev. B*, **40** (1989) 5649–56.
102. Aselage, T. L., Emin, D., Wood, C., Mackinnon, I. & Howard, I., Anomalous Seebeck coefficient in boron carbides. In *Novel Refractory Semiconductors*, ed. D. Emin, T. L. Aselage & C. Wood. MRS, Pittsburg, Pennsylvania, 1987, pp. 27–32.
103. Morosin, B., Aselage, T. L. & Feigelson, R. S., Crystal structure refinements of rhombohedral symmetry materials containing boron-rich icosahedra. In *Novel Refractory Semiconductors*, ed. D. Emin, T. L. Aselage & C. Wood. MRS, Pittsburg, Pennsylvania, 1987, pp. 145–9.
104. Matje, P. & Schwetz, K. A., Surface oxygen pick up in submicron SiC and B_4C sintering powders at room temperature. In *2nd Intern. Conf. on Ceramic Powd. Process. Sci.*, Berchtesgaden, FRG, October 1988, ed. H. Hausner, G. L. Messing & S. Hirano. Deut. Keram. Gesell, Köln, 1989, pp. 377–84.
105. Gogotsi, G. A., Groushevsky, Y. L., Dashevskaya, O. B., Gogotsi, Y. G. & Lavrenko, V. A., Complex investigation of hot-pressed boron carbide. *J. Less Common Met.*, **117** (1986) 225–30.

106. Lavrenko, V. A. & Gogotsi, Y. G., Influence of oxidation on the composition and structure of the surface layer of hot-pressed boron carbide. *Oxid. Met.*, **29** (1988) 193–202.
107. Efimenko, L. N., Lifshits, E. V., Ostapenko, I. T., Snezhko, I. A. & Shevyakova, E. P., Oxidation of hot-pressed boron carbide. *Porosh. Met.*, **4** (1987) 56–60.
108. Makarenko, G. N. & Popova, O. I., Comparative characteristics of phases in the boron–carbon and boron–silicon systems. *J. Less Common Met.*, **117** (1986) 209–14.
109. Pastor, H. & Thévenot, F., Applications industrielles des composés du bore. *Informations Chimie*, **178** (1978) 151–73.
110. Graf von Matuschka, A., *Borieren.* Carl Hanser Verlag, München, Wien, 1977.
111. Goeuriot, P., Thévenot, F. & Driver, J., Surface treatment of steels: Borudif, a new boriding process. *Thin Sol. Films*, **78** (1981) 67–76.
112. Goeuriot, P., Fillit, R., Thévenot, F., Driver, J. & Bruyas, H., The influence of alloying element additions on the boriding of steels. *Mater. Sci. Eng.*, **55** (1982) 9–19.
113. Telle, R., Structure and properties of Si-doped boron carbide. In *NATO Adv. Res. Workshop (ARW), The Physics and Chemistry of Carbides, Nitrides and Borides*, Manchester, UK, September, 1989, Kluwer, ibid ref. 43, pp. 249–67.
114. Murgatroyd, R. A. & Kelly, B. T., Technology and assessment of neutron absorbing materials. *Atomic Energy Rev.*, **15** (1977) 1–74.
115. Tsagareishvili, G. V., Thermal expansion of boron and boron carbide. *J. Less Common Met.*, **117** (1986) 159–61.
116. Telle, R., Boride—eine neue Hartstoffgeneration? *Chemie unserer Zeit*, **22** (1988) 93–9.
117. Hollenberg, G. W., Thermally induced stresses and fractures in boron carbide pellets. *Ceram. Bull.*, **59** (1980) 538–41, 548.
118. Stull, D. R. & Prophet, H., *Janaf Thermochemical Tables*, 2nd edn. National Bureau of Standards, US Government Printing Office, Washington, 1971.
119. Lockwood, A., Elwell, R. & Wood, C., Advanced high temperature thermoelectrics for space power. In *Proc. 16th, Intersoc. Energy Convers. Engineering Conf.*, Vol. 2, 1981, pp. 1985–90.
120. Wood, C., Transport properties of boron carbide. In *Boron-Rich Solids, AIP Conf. Proc. 140*, ed. D. Emin, T. Aselage, C. L. Beckel, I. A. Howard & C. Wood. Amer. Inst. Phys., New York, 1986, pp. 206–15.
121. Türkes, P. R. H., Swartz, E. T. & Pohl, R. O., In *Boron-Rich Solids, AIP Conf. Proc. 140*, ed. D. Emin, T. Aselage, C. L. Beckel, I. A. Howard & C. Wood. Amer. Inst. Phys., New York, 1986, pp. 346–61.
122. Wood, C., Boron carbides as high temperature thermoelectric materials. In *Boron-Rich Solids, AIP Conf. Proc. 140*, ed. D. Emin, T. Aselage, C. L. Beckel, I. A. Howard & C. Wood. Amer. Inst. Phys., New York, 1986, pp. 362–72.
123. Aselage, T., Emin, D. & Wood, C., Thermoelectric properties of boron carbides. *Trans 6th Symp. on Space Nuclear Power*, Albuquerque, NM, 8–12 January 1989, pp. 430–3.
124. Bouchacourt, M. & Thévenot, F., The correlation between the thermoelectric properties and stoichiometry in the boron carbide phase B_4C–$B_{10.5}C$. *J. Mater. Sci.*, **20** (1985) 1237–47.
125. Thévenot, F. & Bouchacourt, M., Propriétés thermoélectriques de la phase carbure de bore. *Silicates Industries*, **49**, (1984) 145–9.
126. Moss, M., Thermal conductivity of boron carbides. *Mater. Res. Soc. Symp. Proc.*, **97** (1987) 77–82.
127. Beauvy, M., Thermal shock resistance of hot-pressed boron carbide. *Sci. Ceram.*, **11** (1981) 385–90.
128. Emin, D., Electronic transport in boron carbides. In *Boron-Rich Solids, AIP Conf. Proc. 140*, ed. D. Emin, T. Aselage, C. L. Beckel, I. A. Howard & C. Wood. Amer. Inst. Phys., New York, 1986, pp. 189–205.
129. Emin, D., Electronic transport in boron carbides. In *Boron-Rich Solids, AIP Conf. Proc. 140*, ed. D. Emin, T. Aselage, C. L. Beckel, I. A. Howard & C. Wood. Amer. Inst. Phys., New York, 1986, pp. 189–205.
130. Emin, D., Theory of electronic and thermal transport in boron carbides. In *NATO Adv. Res. Workshop (ARW), The Physics and Chemistry of Carbides, Nitrides and Borides*, Manchester, UK, September 1989. Kluwer, ibid ref. 43, pp. 691–704.
131. Lipp, A. & Schwetz, K., Härte und Härtebestimmung von nichtmetallischen Hartstoffen. *Ber. Deutsch Keram. Ges.*, **52** (1975) 335–8.
132. Allen, R. D., The solid solution series, boron–boron carbide. *J. Am. Chem. Soc.*, **75** (1953) 3582–3.
133. Bouchacourt, M., Thévenot, F. & Ruste, J., Etudes sur le carbure de bore. I. Métallographie et microdureté Knoop du carbure de bore. *J. Less Common Met.*, **59** (1978) 119–30.
134. Rey, J., Male, G., Kapsa, P. & Loubet, J. L., Boron carbide coatings: correlation between mechanical properties and L.P.C.V.D. parameters values. In *Proc. 7th Eur. Conf. CVD*, Perpignan, France, June 1989.
135. Niihara, K., Nakahira, A. & Hirai, T., The effect of stoichiometry on mechanical properties of boron carbide. *J. Am. Ceram. Soc.*, **67** (1984) C13–C14.
136. Gogotsi, G. A., Firstov, S. A., Vasil'ev, A. D., Gogotsi, Y. G. & Kovylyaev, V. V., Mechanical properties and special features of the structure of materials based on boron carbide. *Porosh. Met.*, **7** (1987) 84–90.
137. De With, G., Note on the temperature dependence of the hardness of boron carbide. *J. Less Common Met.*, **95** (1983) 133–8.
138. Pilyankevich, A. N., Britun, V. F., Tkachenko, Y. G. & Yulyugin, V. K., Structure of boron carbide surface layers after abrasion at 20–1400°C. *Porosh. Met.*, **8** (1986) 93–7.
139. Tkachenko, Y. G., Yurchenko, D. Z., Yulyugin, V. K., Molyar, V. N., Murzin, L. M. & Lugovskaya, E. S., High temperature friction and certain properties of hot-pressed boron carbide. *Porosh. Met.*, **12** (1984) 41–3.
140. Tkachenko, Y. G., Yurchenko, D. Z. & Yulyugin, V. K., Some features of the deformation and fracture of carbides, borides, and nitrides under friction in the temperature range 20–1400°C. *J. Less Common Met.*, **117** (1986) 271–5.
141. Kingon, A. I., Stone, N. A. & Carr, N. S., Performance of some zirconia-based ceramics under conditions of particle erosion. *Mater. Sci. Monogr.*, **38C** (1987) 2657–66.
142. Osipov, A. D., Ostapenko, I. T., Slezov, V. V., Tarasov, R. V., Podtykan, V. P. & Kartsev, N. F., Effect of porosity and grain size on the mechanical properties of hot-pressed boron carbide. *Porosh. Met.*, **1** (1982) 63–7.
143. De With, G., High-temperature fracture of boron carbide:

experiments and simple theoretical models. *J. Mater. Sci.*, **19** (1984) 457–66.
144. Beauvy, M., Propriétés mécaniques du carbure de bore fritté. *Rev. Int. Htes Tempér. Réfr.*, **19** (1982) 301–10.
145. Gogotsi, G. A., Gogotsi, Y. G. & Ostrovoj, D. Y., Mechanical behaviour of hot-pressed boron carbide in various atmospheres. *J. Mater. Sci. Lett.*, **7** (1988) 814–16.
146. Hollenberg, G. W. & Walther, G., The elastic modulus and fracture of boron carbide. *J. Am. Ceram. Soc.*, **63** (1980) 610–13.
147. Ramana Murthy, S., Elastic properties of boron carbide. *J. Mater. Sci. Lett.*, **4** (1985) 603–5.
148. Knoch, H., Carbide-hochverschleißfeste keramische Sonderwerkstoffe. *Techn. Mitt.*, **80** (1987) 221–6.
149. Wilkins, M. L., Use of boron compounds in lightweight armor. In *Boron and Refractory Borides*, ed. V. I. Matkovich. Springer Verlag, Berlin, 1977, pp. 633–48.
150. Epik, A. P., Boride coatings. In *Boron and Refractory Borides*, ed. V. I. Matkovich. Springer Verlag, Berlin, 1977, pp. 597–612.
151. Hunold, K., Boron carbide/graphite thermocouple for high temperatures. *Chem. Tech. (Heidelberg)*, **14** (1985) 82–4.
152. Hunold, K., A thermocouple for high temperatures. *Adv. Mater. Process.*, **9** (1986) 4–5.
153. Kanno, Y., Temperature control of inert gas furnace by tetraboron carbide/carbon thermocouple. *Yogyo Kyokaishi*, **94** (1986) 449–51.
154. Reinmuth, K., Lipp, A., Knoch, H. & Schwetz, K. A., Borhaltige keramische neutronenabsorberwerkstoffe. *J. Nucl. Mater.*, **124** (1984) 175–84.
155. Colin, M., Matériaux absorbants neutroniques pour le pilotage des réacteurs nucléaires. In *Techniques de l'ingénieur Génie nucléaire–Structure des réacteurs nucléaires*, Paris, 1989, Vol. 2, **B3720**, pp. 1–8.
156. Kryger, B., 1989, pers. commun.
157. FBFC, Nuclear fuel fabrication. Document, Romans, France, June 1986.
158. Halverson, D. C., Pyzik, A. J. & Aksay, I. A., Processing and microstructural characterization of B_4C–Al cermets. *Ceram. Eng. Sci. Proc.*, **6** (1985) 736–44.
159. Pyzik, A. J., The role of rearrangement in the densification of ceramic–metal composites under hydrostatic pressure. In *2nd Intern. Conf. on Ceramic Powd. Process. Sci.*, Berchtesgaden, FRG, October 1988, ed. H. Hausner, G. L. Messing & S. Hirano. Deut. Keram. Gesell., Köln, 1989, pp. 783–92.
160. Halverson, D. C., Pyzik, A. J., Aksay, I. A. & Snowden, W. E., Processing of boron carbide–aluminium composites. *J. Am. Ceram. Soc.*, **72** (1989) 775–80.
161. Bougoin, M., Thévenot, F., Dubois, J. & Fantozzi, G., Synthèse et propriétés thermomécaniques de céramiques denses composites carbure de bore–carbure de silicium. *J. Less Common Met.*, **132** (1987) 209–28.
162. Dubois, J., Fantozzi, G., Bougoin, M. & Thévenot, F., Microstructure et propriétés mécaniques de matériaux, de types B_xC/SiC frittés, sans charge. *J. Phys. Colloque C1, Suppl. No. 2*, **47** (1986) C1-751-5.
163. Wei, G. C., Silicon carbide whiskers-reinforced ceramic composites and method for making same. US Patent 4 543 345, 1985.